

A Simplified Heat Wave Warning System

Arya Nakhaie Ashtiani

A Thesis

in

The Department

of

Building, Civil and Environmental Engineering

Presented in Partial Fulfillment of the Requirements

for the Degree of Master of Applied Science (Building Engineering) at

Concordia University

Montreal, Quebec, Canada

April 2013

© Arya Nakhaie Ashtiani, 2013

CONCORDIA UNIVERSITY
School of Graduate Studies

This is to certify that the thesis prepared

By: Arya Nakhaie Ashtiani

Entitled: A Simplified Heat Wave Warning System

and submitted in partial fulfillment of the requirements for the degree of

Master of Applied Science (Building Engineering)

complies with the regulations of the University and meets the accepted standards with respect to originality and quality.

Signed by the final examining committee:

Dr. H. Akbari Chair

Dr. K. Khorasani Examiner

Dr. L. Wang Examiner

Dr. F. Haghighat Supervisor

Approved by _____
Chair of Department or Graduate Program Director

Dean of Faculty

Date _____

Abstract

A Simplified Heat Wave Warning System

Arya Nakhaie Ashtiani

Extreme heat is a natural hazard that could rapidly increase in frequency, duration, and magnitude in the 21st century. During the summer, the combined effect of urban heat island (UHI), climate change and global warming increases ambient air temperature. This leads to a rise in indoor environment temperature, reduction of thermal comfort, increase of cooling demand, and heat related morbidity and mortality especially among vulnerable people such as the elderly and those who are living in buildings without mechanical ventilation systems.

Cities are developing tools to predict the indoor air temperature during extreme heat waves in order to be able to provide emergency plans if necessary. To do so, it is required to find a relationship between the indoor and outdoor conditions. Hence there is an urgent need to develop a reliable method for indoor air temperature prediction by taking into consideration not only the outdoor conditions but also the socio-economic aspects of the neighborhood.

The objective of this study is to develop a warning system to predict the indoor air thermal condition during heat wave events in buildings without mechanical ventilation systems. In order to develop a regional heat warning system, two different methods were proposed and tested for an indoor air temperature forecasting application with respect to neighborhood parameters. The first method was based on regression and the second one was based on the Artificial Neural Network (ANN) model. The inputs and outputs to the

proposed models were the field measurement data which has been collected on Montreal Island during the summer of 2010 (Park et al, 2010). To find the most practical approach, both proposed models were compared with respect to their accuracy and the required resources. A comparison of the proposed regression and ANN models was conducted by two different levels of simulation. The ANN model showed better accuracy in predicting the indoor dry-bulb temperature, but it was more complicated to apply.

AKCOWLEDGEMENT

I would like to express my sincere appreciation to my advisor, Dr. Fariborz Haghghat, for giving me the opportunity to pursuit my Master's degree and for his wisdom, continuous support, motivation, and immense knowledge during my graduate studies. His guidance was a great asset, without which this research would not been possible.

Beside my supervisor, I would also like to express my love and gratitude to my parents and sisters for their endless love, care, and support. And finally to my friends and colleagues, especially Behrang Talebi and Behzad Rouhieh for their help, I really appreciate it.

Table of Contents

List of Figures.....	ix
List of tables.....	xi
List of Abbreviations	xii
Chapter 1	1
Introduction.....	1
1.1 Urban Heat Island (UHI)	1
1.2 Climate Change and Global Warming	3
1.3 Heat Watch/Warning Systems	6
1.4 Heat/Health Warning System Development in Toronto and Montreal.....	9
1.5 Objective and scope of work.....	10
Chapter 2	12
Literature Review.....	12
2.1 Introduction.....	12
2.2 Methods for Air Temperature Prediction.....	13
2.2.1 Application of Regression Models for Indoor Air Temperature Prediction	13
2.2.2 Application of Artificial Neural Networks (ANN) for Indoor Air Temperature Prediction.....	15
2.2.3 Application of Regression Models for Outdoor Air Temperature Prediction.....	17
2.2.4 Application of Artificial Neural Networks for Predicting Outdoor Air Temperature	18
2.3 Influential Parameters on Indoor Temperature	22
2.3.1 Outdoor Dry-bulb Temperature	23
2.3.2 Solar Radiation.....	23
2.3.3 Local Wind Velocity.....	24
2.3.4 Relative Humidity	25
2.3.5 Location of indoor temperature measurement	25
2.3.6 Vegetation Ratio	25
2.3.7 Aspect Ratio (Urban and Building Geometry)	26
2.3.8 Occupancy.....	26
2.3.9 Time of the day	27
2.3.10 Building Volume.....	27

2.3.11 Other Factors.....	28
Chapter 3	29
Measurements	29
3.1 Measurements and Localization.....	29
3.2 Study Area	29
3.3 Data.....	30
Chapter 4	38
Methodology	38
4.1 Model Validation Criteria	38
4.2 Input Data and Variables	38
4.2.1 Building Height.....	39
4.2.2 Wind Effect.....	40
4.2.3 Aspect Ratio.....	41
4.2.4 Building Volume and Occupancy	41
4.2.5 Vegetation and Albedo	42
4.2.6 Sensor Location	42
4.2.7 Solar Heat Gain.....	42
4.2.8 Sol-air Temperature	44
4.3 Input Data Processing	45
4.3.1 Linear Regression	51
4.3.2 Multiple Linear Regressions (MLR).....	51
4.3.3 Time Series	52
4.3.4 Multiple Non-Linear Regression (MNL)	53
4.3.5 Artificial Neural Network (ANN).....	54
Chapter 5	57
Analysis, Results, and Discussion	57
5.1 Time Series	57
5.1.1 Apply the method.....	57
5.1.2 Level 1 Simulation.....	58
5.1.3 Level 2 Simulation.....	61
5.2 Artificial Neural Networks	62
5.2.1 Apply the method.....	62

5.2.2	Level 1 Simulation.....	63
5.2.3	Level 2 Simulation.....	65
5.3	Model Comparison.....	66
	Chapter 6	68
	Conclusions and Recommendations	68
6.1	Concluding Remarks.....	68
6.2	Recommendations for Future Work.....	70
	References.....	72

List of Figures

Figure 3.1 (a) High surface temperatures, (b) high population density, (c) socio-economically deprived areas, and (d) minimal vegetation.....	32
Figure 3.2 Location of buildings under study	33
Figure 3.3 Hourly maximum and minimum indoor thermal conditions during first heat wave	34
Figure 3.4 Hourly maximum and minimum indoor thermal conditions during second heat wave	35
Figure 3.5 Hourly indoor dry-bulb temperatures of BLDG9 & BLDG10 during July 1st to July 20th	36
Figure 4.1 Wind speed at airport, downtown, and other sample areas of study	47
Figure 4.2 Measured indoor dry-bulb temperature for buildings no. 28, 19, 37 (BLDG28, BLDG19, BLDG37)	50
Figure 4.3 Measured indoor dry-bulb temperature for buildings no. 25, 19, 37 (BLDG25, BLDG19, BLDG37)	50
Figure 4.4 Basic structure of 3-layer feed forward neural network with multiple inputs and a single output.....	56
Figure 5.1 Simulated hourly indoor dry-bulb temperatures of units in zone (a).....	60
Figure 5.2 Simulated hourly indoor dry-bulb temperatures of units in zone (a).....	60
Figure 5.3 Simulated hourly indoor dry-bulb temperatures of units in zone (a).....	61
Figure 5.4 Simulated hourly indoor dry-bulb temperatures of units in zone (a) by artificial neural network model	64
Figure 5.5 Simulated hourly indoor dry-bulb temperatures of units in zone (a) by artificial neural network model	64
Figure 5.6 Simulated hourly indoor dry-bulb temperatures of units in zone (a) by artificial neural network model	65

Figure 5.7 Predicated results of ANN and Time Series models correspond to simulation level 2 67

List of tables

Table 3.1 Regions under study on the Island of Montreal	33
Table 3.2 Sample measured data	37
Table 4.1 Characteristics of under studied buildings	46

List of Abbreviations

Abbreviation	Stands for
ANN	Artificial Neural Network
BLDG	Building
LR	Linear Regression
MLR	Multiple Linear Regression
MNLR	Multiple non-Linear Regression
MSE	Mean Square Error
RBF	Radial Basis Function
RMSE	Root Mean Square Error
TPH	Toronto Public Health
UHI	Urban Heat Island
UHII	Urban Heat Island Intensity

Chapter 1

Introduction

1.1 Urban Heat Island (UHI)

Due to the increase in urbanization, industrialization, and human activities, especially after the Second World War, cities experience higher temperatures than their nearby rural areas. This phenomenon, known as Urban Heat Island (UHI), is being investigated worldwide, and first was documented by Luke Howard in 1818 (Mirzaei and Haghghat 2010; Sailor and Dietsch, 2007). The phenomena of UHI is already documented in many cities i.e., London (Chandler, 1965), Montreal Island (Oke and East, 1971), Toulouse (Estournel et al., 1983), Paris (Escourrou, 1991), Mexico (Oke et al., 1999), and Atlanta (Bornstein and Lin, 2000).

The undesired side effects of UHI on decreasing outdoor air quality, increasing air conditioning energy consumption, heat related illness and mortality make it a hazardous issue that motivates scholars to study its influential parameters, mitigation strategies and prediction methods. Heat waves rank first as the cause of human mortality compared to other meteorological hazards i.e., floods, hurricanes, and tornadoes. It poses threats to property and human health (Wilhelmi et al., 2004). Hajat et al. (2002) defined heat wave as a three day rolling average above the 97th percentile value of 21.5° C.

Studies showed that heat can aggravate medical problems particularly with the elderly, children, and the ill (Smoyer 1998; Nakai et al. 1999). Hospitalizations were increased in London and Chicago during the 1995 heat waves (Rooney et al., 1998;

Semenza et al., 1999). People suffering from cardiovascular, cerebrovascular, and respiratory diseases experience an increase in overall mortality during and following heat waves (Kilbourne 1997). The human physiological response to excessive heat entails an increase in surface blood circulation, in order to increase heat loss through radiation, convection, and increased rates of evaporative cooling by sweating (Bouchama & Knochel, 2002). An increase in cardiac output is needed to increase circulation, but is limited by maximum heart rate and vascular volume. Under excessive levels of heat stress, the body can no longer maintain temperature balance and death may occur (Sheridan and Kalkstein 2004).

The National Weather Service Office of Climate, Water, and Weather Services estimated that a total of 2,248 people throughout the United States lost their lives due to extreme heat waves between 1986 and 2000. Moreover, they estimated 2,200 million dollars were lost to extreme heat weather during the same period (Wilhelmi et al., 2004). The deaths of around 50,000 people in August 2003, in Europe is the recent example of a heat wave contributing to mortality (Mirzaei and Haghightat 2010).

In addition to above information, UHI affects the indoor thermal environment conditions such as temperature and humidity especially in dwellings where HVAC systems and mechanical ventilation systems are not available (Health Canada, 2009). Therefore, studying the UHI phenomena can be useful to improve indoor thermal conditions prediction. By considering the fact that the vulnerable groups of people may spend more time in their places during the day (Oikonomou et al., 2012), knowing the indoor thermal conditions (instead of outdoor thermal conditions) may help city planners to provide better

emergency plans for vulnerable people. A better emergency plan leads to an improvement in human health survival by reducing morbidity and mortality.

Moreover, knowing the indoor air temperature is important to evaluate the strict thermo-hygrometric environment in museums (Ascione et al., 2009). Balaras et al. (2007) reported that an accurate knowledge of the room temperature required assessing the indoor air quality of hospital operating rooms for patients and medical persons. Also, the knowledge of room temperature is required to analyze the thermal comfort and indoor air quality evaluation of naturally ventilated buildings (Yan et al., 2008; Wei et al., 2011).

1.2 Climate Change and Global Warming

Climate change is induced by anthropogenic heat and greenhouse gases and results in global warming. Both climate change and global warming derange the local or regional climate by way of heat trapping. They not only result in extreme weather formation, but also increase the intensity of extreme weather events. Moreover, the effect of urbanization and industrialization on the quality of the environment is multiplied. The problems of high summer temperatures in urban areas are likely to become worse in the future because of climate change (Oikonomou et al., 2012). The climate change induced by the emissions of greenhouse gases is considered as one of the main challenges facing human kind in the 21st century with serious global consequences for the environment and human health. Climate change is felt to be more important in countries that might experience a shift from predominantly heating to predominantly cooling of their buildings (Guan, 2012; Wilde & Coley, 2012).

Global warming is the rise in the average temperature of the Earth's surface, atmosphere, and oceans and its projected continuation. It is primarily caused by increasing concentrations of greenhouse gases (Choices Committee on America's Climate; Council National Research. 2011). It is certain that global warming can increase the frequency and intensity of heat waves which can cause discomfort to the human body and, in the worst case scenario, can lead to more heat illness casualties (Lun et al., 2012). Lun et al, (2012) stated that there is an interrelationship between extreme weather, climate change, and global warming.

The frequency and severity of extreme weather events, such as heat waves, are projected to increase as a result of climate change. Global warming trends are projected to double the likelihood of such events (Mavrogianni et al., 2012). Current projections suggest a heat wave of similar magnitude of summer 2003 may occur as frequently as every three years by the 2050s (Hajat et al., 2007; UKCIP 2010; Pachauri and Reisinger 2007).

It is also expected that climate change increases the risk of overheating in buildings. Buildings provide an interface between the outdoor environment, which is subjected to climate change, and the indoor environment, which needs to remain within a specific range to keep the building occupants comfortable and healthy.

Buildings, as one of the most significant factors, contribute to the global warming process by consuming a considerable amount of energy and materials (Guan 2011). Buildings are responsible for 40% of the world's total energy use, 30% of raw materials consumption, 55% of timber harvests, 16% of fresh water withdrawal, 35% of global carbon dioxide (CO₂) emissions and 40% of municipal solid waste sent to landfills (Fenner

& Ryce, 2008). Also, Buildings are considered to be the main contributor to the UHI effect. Building masses increase the thermal capacity, decrease water evaporation by reducing green areas, and lessen wind velocity at ground level by increasing ground surface roughness. Therefore buildings have a direct bearing on city ventilation and temperature and are intensive energy consumers and a major cause of greenhouse gas emissions (Lun et al., 2012). Several modeling case studies also showed that there is high risk of thermal discomfort and heat stress due to climate change in many existing buildings (CIBSE 2005). However, the impact of climate change is largely dependent on several building characteristics and environmental factors such as the height of the buildings and vegetation ratio that will be discussed further.

Wilde and Coley (2012) extensively discussed the climate change impact on the urban area. The overall conclusion of their study articulated that the impact of climate change results in an increase in indoor air temperature, especially in buildings in temperate climates. Gupta and Gregg (2012) assessed the effect of future temperature change in existing English homes. They found out that, ultimately among the passive options tested, none could completely eliminate the risk of overheating in the homes, particularly by the 2080s.

As mentioned before, high indoor temperatures in dwellings can have adverse effects on energy use, comfort and health. The dynamic interaction between building systems and external climate is extremely complex, including a large number of complicated variables and phenomena. It is important to develop a simple approach to determine indoor temperatures using forecasted weather data which will be discussed further in this thesis.

1.3 Heat Watch/Warning Systems

Heat is rated as the greatest weather killer factor in many areas of the world. Considering the growing numbers of vulnerable people (elderly and children) and increasing social isolation, significant number of people will be susceptible to heat waves. Moreover, in a potentially warmer world, heat susceptibility could increase further (Kalkstein and Greene 1997). Thus, in order to protect the public and especially vulnerable persons from heat, establishing heat watch-warning systems and mitigation plans is necessary.

In many cities, the primary heat alert systems were based on the computation of the heat index, which combines the impact of temperature and relative humidity. In Philadelphia, a heat warning was issued when daytime heat index values were expected to reach 40.5 °C or above for more than 3 hours a day for 2 consecutive days, or when the daytime heat index is expected to exceed 46 °C for any length of day (Kalkstein et al., 1996; NOAA 1994). For years, the US National Weather Service issued warnings when a daytime heat index reached 41°C or above with nighttime lows at or above 27 °C for two consecutive days (NWS 1992). In Shanghai excessive heat warnings were issued by the Meteorological Bureau on days in which the maximum temperature exceeded 35 °C (Tan et al., 2004).

The systems designed based on heat index contain some disadvantages. First, these systems consider the effect of only two meteorological variables on people (temperature and humidity). It is quite clear from other studies that a number of other meteorological variables play a significant role on human comfort, like wind and radiation (Kalkstein and

Davis 2005; Steadman 1979). Second, it does not take into account the fact that earlier summer heat waves of similar character often create more of a health danger than those late in the season (Kalkstein 1993; Kalkstein and Greene 1997). Third, they are not able to estimate mortality or morbidity that are a consequence of heat waves. Finally, these systems were used in many locations without considering human adaption and acclimatization (Kalkstein and Valimont 1986).

The fact that the human body responds to the total effect of all-weather variables interacting simultaneously on it rather than to individual meteorological elements, encourages researchers to design more effective heat watch/warning systems. In Philadelphia a heat alarm system based on a climatological index was developed to categorize each day based on its meteorological character. Air temperature, dew point temperature, total cloud cover, sea level pressure, wind speed, and wind direction were six meteorological elements which were used for developing the system and classifying days into some meteorologically homogeneous (air mass) categories. The system forecasts air mass types of the current day and coming 2 days. The air mass types are mostly as follows (Sheridan and Kalkstein 2008; Tan et al., 2004):

- Dry polar: very cold, very dry
- Dry moderate: mild, dry
- Dry tropical: very hot, very dry
- Moist polar: cold, cloudy, rainy
- Moist moderate: overrunning, cool, drizzle, fog
- Moist tropical: hot, very humid
- Transition: a change from one air mass type to the next

A standard stepwise multiple regression analysis was then used to determine which factors within the oppressive air mass contribute to elevated mortality. In Philadelphia and many other cities these factors were recognized as the number of consecutive days the oppressive air mass had been present, and the time of season that the heat wave occurred. Among those, the air masses that contain both highest average temperature and humidity, and dew point in some cases like dry tropical and moist tropical, were considered as the most oppressive air mass types (Kalkstein et al., 1996; Sheridan and Kalkstein, 2004). The new warning systems alert the public more effectively to offensive days when dangerous weather is predicted, thus saving more lives (Tan et al., 2004).

Ebi et al. (2004) concluded that issuing a warning lowered daily mortality by about 2.6 lives on average. It implies that the gross benefits of the Philadelphia Hot Weather-Health Watch/Warning System which was developed in 1995 could be on the order of 468 million dollars (117 lives saved) over the 3 year period (1995 - 1998). The low estimated cost of heat warning systems argues for being more tolerant about issuing warnings. The total cost of the Philadelphia heat warning system was in the order of 210 thousand dollars over the same period. Obviously, if such heat warning system saved any lives, it would have large estimated dollar benefits. This is because the value of a statistical life (VSL), for even one life, is bigger than the cost of the system. It is also noteworthy that morbidity reduction is an additional benefit which was not included in their analyses. Tan et al. (2004) analyzed a warning system for Shanghai throughout the summer of 1999. The algorithm predicted 331 excess deaths due to the heat wave, only slightly more than 294 recorded.

The heat warning system of Philadelphia has been the basis for many other heat warning systems (Kalkstein 2002; Sheridan and Kalkstein 1998). Over the past several

years, many more synoptic based systems were developed and improved in other United States cities including Phoenix, Arizona; Washington, D.C.; Chicago, Illinois; St. Louis, Missouri; Cincinnati and Dayton, Ohio, and a network of cities across Tennessee, Louisiana, Arkansas, and Mississippi. Also, systems were developed for cities in other countries including four Italian cities; Toronto, Ontario; (Canada) and Shanghai, (China) (Sheridan and Kalkstein 2004).

1.4 Heat/Health Warning System Development in Toronto and Montreal

It was about the beginning of the 21st century that Canadian cities began to develop programs to protect the public from heat waves. Toronto and Montreal are the largest urban centers in Canada. Various climatological, demographic, environmental, and socio-economic factors threaten the population of the two cities by imposing the risk of mortality and morbidity during summertime (Smoyer-Tomic and Rainham 2001).

In 1999, Toronto Public Health (TPH) set a warning system that issued an alert when humidex (which is an index calculated from dry-bulb temperature and humidity) reached 40°. The emergency services implemented through hospitals and other institutions when humidex reached 45°. During the period 1998-2003, Montreal Public Health Authority had become active in order to respond and appropriately deal with summer heat waves. As a part of Montreal's heat response plan, public warnings were issued whenever a temperature of 30° C or more and an apparent temperature of 40° humidex or more were forecasted (Kosatsky et al., 2005).

In 2000, based on the requirements of TPH and Toronto Atmospheric Fund, the University of Delaware and Dr. Lawrence Kalkstein developed a more predictive heat/health warning system for Toronto. The new system is based on the retrospective analysis of 17 years of daily mortality in relation to weather factors. In 2003, a research was conducted in Montreal to identify the weather parameters associated with excess mortality using both time series and synoptic approaches. Based on that research, the action level for issuing alert systems for the following summers were modified (Kosatsky et al., 2005).

1.5 Objective and scope of work

Extreme heat is a natural hazard that could rapidly increase in frequency, duration, and magnitude in the 21st century. This would lead to increase discomfort, with implications for health, and mortality. The combination of increasing urbanization, growing numbers of vulnerable people, such as the elderly and children, and the evidence of global warming and climate change indicate an urgent need for improved simplified heat wave response systems. Sheridan and Kalkstein (2009) mentioned that even with outdoor temperatures remaining similar from day to day during a heat wave, indoor temperature may continue to escalate, creating an excessive health hazard. As mentioned before, using the indoor temperature in heat watch/warning systems may lead to improving the system prediction and decreasing the rate of heat mortality/morbidity.

To date, there are two types of models for predicting room air temperature: analytical (simulation) and numerical (statistical) models. Limited research has been carried out that explores the use of different statistical methods in predicting indoor air

temperature during heat wave in the UHI. On the other hand, so many different building simulation programs exist but most of them are complex and require detailed information about physical building characteristics (Lankester and Brimblecombe, 2011). The statistical methods are much simpler and quicker in prediction.

The objective of this thesis is to develop a warning system using two different types of statistical methods: regression and ANN. This system is expected to predict the indoor air thermal condition in buildings occupied by most vulnerable people (low income, hot spot, highly populated) during heat waves. The existing field measurement data that was carried in Montreal in 2010 was used. These two methods (regression and ANN) are proposed and tested for indoor air temperature forecasting application with respect to ambient weather conditions and UHI effects.

Chapter 2

Literature Review

2.1 Introduction

Wu and Su (2012) stated, in general, there are two types of models for predicting room air temperature: analytical and numerical models. The analytical models are widely implemented in popular simulation tools such as EnergyPlus (Pedrini 2002), DOE-2, TRANSYS, Modelica (Wetter 2009), eQUEST, etc. These models are complex, because they use detailed architectural and building materials properties parameters to describe the thermal phenomena processes. This is very important since architectural and material parameters of a building greatly influence its thermal performance. These models can be used to predict indoor thermal environment at early stage of design, even before the building is constructed. However, Lowry and Lee (2009) presented that there are many simplifying assumptions that make it quite a challenge to obtain reliable analytical models. These assumptions are made to deal with complexity of thermal interactions, unmeasured disturbances, uncertainty in thermal properties of structure elements and other parameters. This is also a time consuming process since requires extensive input data.

In addition, numerical data-driven modeling approaches establish models by only using input and output measurements (Wu and Su, 2012). Thus, they are time-efficient methods due to their simple structure. They also have low computation cost compared to analytical models. But, these models are highly dependent on the measurements. Artificial Neural Networks (ANN), and regression methods are two numerical approaches. Many

researchers have developed numerical models for the indoor air temperature prediction. For this purpose, they used observations. Field measurements and thermal remote sensing are two different observation methods (Mirzaei and Haghighat, 2010).

2.2 Methods for Air Temperature Prediction

With recent progress in computational tools, simulation methods and computational techniques have been used extensively to solve large scale problems. However, the complexities of air temperature prediction, the increased cost and required computational time of the analytical modeling approaches have led to the exploration of other accurate prediction methods. All these approaches have their own limitations and drawbacks. They are not able to take into consideration all the phenomena and parameters that simultaneously affect the indoor air temperature (Mirzaei and Haghighat, 2010; Gobaksi et al., 2011).

2.2.1 Application of Regression Models for Indoor Air Temperature Prediction

The linear regression model has been widely used for predicting and forecasting (ASHRAE Fundamentals, 2009). Linear regression assumes there is a direct linear correlation between variables. This assumption is sometimes incorrect. Outliers, the observations that are distant from the rest of data, can have huge effects on the linear regression by decreasing the accuracy of the prediction since extreme values cannot be always captured in the predictions.

Lankester and Brimblecombe (2011) used this model to predict indoor air temperature and relative humidity in unheated historic rooms across Europe. The historic room in this study is a place where antiques are kept. In their study, the daily outdoor temperature is the input and the daily indoor temperature is the output of the model. Different coefficients were determined for each month to consider the seasonal variation in building ventilation. These coefficients were derived from 9 years of observations of room thermal condition and outdoor weather conditions. Although the value of R^2 (the coefficient of determination) was 0.93, the model failed to capture the extreme values. The main drawback of the regression technique is that it is case specific. That means the model is only good for the room that the data was used to develop and cannot be used for other rooms.

Wright et al., (2005) indicated that, clearly there is a relationship between indoor and outdoor air temperature. This correlation can be shown by plotting daily average indoor air temperature against daily average outdoor air temperature with different relationships for different rooms. They conducted a study in UK to predict indoor temperature in a sample of residential dwellings during august 2003. They found the R^2 values of 0.78 and 0.73 for bedroom and lounge, respectively. The above studies did not consider the effect of other meteorological parameters as well as local environmental factors and building characteristics.

Wright et al. (2005) also stated since buildings have thermal mass, in order to analyze the indoor air temperature the history of outdoor air temperature over a few days, should be taken into consideration. As a matter of fact, there is a better correlation between

indoor air temperature and outdoor air temperature of preceding days. To capture the historic influence of outside air temperature, they used the following equation:

$$T_h^n = \alpha T^n + (1 - \alpha) T_h^{n-1} \quad (1)$$

where, T_h is the historic indoor air temperature, T^n is the average outdoor air temperature on day n , and α is a constant between zero and one ($0 < \alpha \leq 1$). α represents the thermal mass of buildings. A linear relationship between T_h and the daily average indoor temperature was established for each room. α was optimized to maximize the R^2 values for each studied room. The linear relationship can later be used for further prediction. The R^2 values were 0.96 and 0.93 for bedroom and lounge, respectively. Moreover, the method was applied to 3 other rooms and similar results were obtained. R^2 values were consistently high, all just over 0.9 showing this was a trustable model. Greater value of α means lightweight materials were used in the building. In their study, values of α range from 0.3 to 0.8, but most values were in the range 0.3 to 0.5.

2.2.2 Application of Artificial Neural Networks (ANN) for Indoor Air Temperature Prediction

Thomas and Mohseni (2007) discussed on how to identify black-box indoor air temperature prediction models in buildings. They carried out the study in two different buildings located in the southern part of Sweden. They used measured data such as internal heat power, indoor air temperature, outdoor air temperature, solar radiation, and time of the day for six days every 10 minutes. Different linear and nonlinear prediction models were identified and compared. They concluded that for the studied buildings, the ANN

models trained by the Levenberg-Marquardt algorithm gave more accurate temperature predictions than linear regression models using the least squares method (MATLAB, 2012). They reported that ANN models are better than linear regression models since they provide more accurate responses when applied to nonlinear systems.

Lu and Viljanen (2009) used ANN to predict the indoor air temperature and relative humidity in a house. Indoor and outdoor temperature and relative humidity were measured every 15 minutes for 30 days. No additional information was considered for the input of the model. In their study, indoor air temperature predictions performed better than those of indoor relative humidity. R^2 values between predicted and measured air temperatures were 0.998 and 0.997 for the air temperature and humidity models, respectively.

Mirzaei et al. (2012) discussed developing reliable tools to predict indoor air temperature using available building characteristics, climate data and socio-economic factors. In their study, two models (simplified and advanced) were developed to predict hourly indoor dry-bulb temperatures in 55 residential buildings. Both models used ANN technique. The simplified model generated a correlation between airport weather observations (outdoor dry-bulb temperature, relative humidity, wind speed, and solar radiation) and monitored indoor dry-bulb temperatures. The advanced model included ten influential parameters, which represented the effect of neighboring environment and building characteristics. These ten input data were: outdoor dry-bulb temperature, relative humidity, neighboring wind speed, solar radiation, building volume, building occupancy, aspect ratio, vegetation ratio, location of indoor temperature measurement, and hour of the day. The output of the model was measured indoor dry-bulb temperature. The advanced model showed better accuracy in predicting the indoor thermal conditions. The MSEs were

2.51 for the advanced model and 2.74 for the simplified model in the last level of validation. It is justifying the use of neighborhood specific parameters to forecast indoor environment condition in an urban heat island area.

Many other researchers have used ANN models to predict indoor air temperature. Pollard and Stoecklein (1998) used ANN models to predict the indoor air temperature of a residential building and compared the results to linear regression methods. They concluded that the results are comparable. Mechaqran and Zouk (2004) compared prediction results of indoor air temperature of a building using ANN and linear regression models. In this case ANN model provided clearly more accurate results. Moreover, prediction of indoor air temperature using ANN models has been discussed by Gouda et al. (2002) and Kalogirou (2000). Mechaqran and Zouk (2003) studied the optimum size of a neural network to predict the indoor air temperature in order to decrease the error. Ferreira et al. (2002) used radial basis function (RBF) ANN models to predict indoor temperature of a greenhouse. Ruano et al. (2006) also used RBF ANN to predict indoor air temperature of a school. Similar work was done by Zhang et al. (2005). These examples provide an insight into the depth of ANN studies in predicting the indoor temperature.

2.2.3 Application of Regression Models for Outdoor Air Temperature Prediction

Priyadarsini et al. (2008) used multiple linear regression (MLR) technique to predict the air temperature inside an urban canyon. The independent variables were: wind speed, aspect ratio (H/W), and surface temperature of the façade materials. Two different scenarios were considered. In the first scenario, the MLR model was used to relate the outdoor air temperature to mentioned independent parameters at very low wind speeds.

The R^2 value was 0.87 that showed a good fit. In the second scenario, different wind speeds were considered and the R^2 value in this case was 0.54 which is a poor fit. It was found that at very low wind speeds, the effect of façade material and their colours was very significant on the air temperature at the middle of a narrow canyon.

Giridharan et al. (2008) employed MLR technique to study the impact of on-site variables on the influence of vegetation in lowering outdoor air temperature. In this study the selected independent variables were: surface albedo, sky view factor, altitude, shrub cover, tree cover, and average height to floor area ratio. The dependent variable for the analysis was the UHI intensity, which is defined as temperature difference between a measurement point in the residential estate and the observatory station at a particular time. For five different scenarios of vegetation level and sky clearness, the R^2 values of daytime model were 0.44, 0.44, 0.57, 0.36 and 0.75. R^2 values of night time model for the same scenarios were 0.58, 0.37, 0.88, 0.24, and 0.74. The regression models used in this study were able to explain the influence of on-site variables on vegetation in lowering the outdoor temperature within the respective urban settings.

2.2.4 Application of Artificial Neural Networks for Predicting Outdoor Air Temperature

Shao et al. (2011) applied artificial neural network to predict heat island effect. The input nodes consisted of solar radiation, precipitation, sunshine duration, the average wind speed, and underlying surface. Among those, underlying surface had four parameters: evaporation rate, thermal conductivity, reflectivity, and heat capacity of the buildings and road materials. The forecast temperature was set as the output node. A feed forward

network with 10 hidden nodes was employed. For this study, meteorological data of a total of 36 months from 1995 to 1997 was used. Finally, in order to verify the effectiveness of this model, Pearson correlation coefficient was used to make correlation analysis between forecast and actual outdoor air temperature. The R^2 value was 0.953 which shows the high capability of the model for air temperature prediction.

Gobakis et al. (2011) developed an ANN model to predict UHI intensity in order to demonstrate the applicability of neural network for UHI intensity prediction. In this study, hourly data collected from April 2009 to September 2009 was used for training and verification of the neural network. In addition to 6 different training functions, the proposed model was tested using Elma, Feed-Forward, and Cascade neural network architecture. The input data (nodes) were: day of the year (1 to 365), time which was converted into minutes of the day (0 to 1380), ambient air temperature measured at different stations ($^{\circ}\text{C}$), and global solar radiation (W/m^2). The output was UHI intensity ($^{\circ}\text{C}$). The results showed that the most suitable ANN architecture for the UHI intensity prediction was the Elman type using Levenberg-Marquardt as transfer function (MATLAB, 2012). The mean square errors (MSE) of the three neural networks were 0.35, 0.65, and 1.12 for Elman, Cascade, and Feed-Forward architectures, respectively.

Kolokotroni et al. (2006) used ANN method to study the effect of synoptic climatic conditions on UHI intensity in London. The inputs were selected as: cloud cover, humidity, wind speed, diffuse radiation, global radiation, ambient air temperature, and radial distance of the ten investigated locations from Central London. The output was selected as the hourly ambient air temperature at specific locations (investigated locations). In this case, a back-propagation Feed-Forward neural network with 'trainsecg' training function was

developed. 19 hidden neurons were chosen by trial and error based on their performance for 24 sets of data sets (MATLAB, 2012). The MSE for training set of data was about 0.2 and for testing set of data (untrained) was about 0.35.

Mihalakakou et al. (2002) employed ANN method to study and simulate UHI over Athens in a considerable number of locations (23 stations for a period of 2 years). The network was trained using hourly measured ambient air temperature at reference and another station (2 inputs), synoptic scale atmospheric circulation, maximum daily values of total solar radiation, and mean daily values of wind speed as input neurons. In this study, a multilayered neural network based on back-propagation algorithm was implemented for each of the 23 locations to predict UHI intensity. Every network consisted of one hidden layer of 20 to 25 neurons. Untrained data of 230 days in 1998 was used to test the results. The results for the measured data were in strong correlation with the estimated data for the whole set of testing data. The root mean square errors ranged from 0.1°C to 0.3 °C.

Kim and Baik (2002) tried to find the relationship between UHI intensity and meteorological elements in Seoul using a MLR model. They developed a three layer feed forward back-propagation neural network and multiple non-linear regression (MNL) models (power and quadratic) for forecasting UHI intensity. They demonstrated the potential of the ANN model in predicting UHI intensity by comparing its performance with the non-linear regression models. The independent variables (input nodes for ANN model) were: maximum UHI intensity for the previous day, wind speed, cloudiness, and relative humidity which were measured at two meteorological stations at six hours intervals. The dependent variable or output node for the ANN model was the UHI intensity. UHI intensity was defined as the maximum temperature difference between Seoul and Yangpyong. The

R^2 values for MLR, power MNLR, and quadratic MNLR models were 0.461, 0.381, and 0.463, respectively. However, for the test dataset, the average prediction errors for the ANN, MLR, power MNLR and quadratic MNLR are 1.18 °C, 1.26 °C, 1.34 °C, and 1.23 °C, respectively. It was concluded that the reason for the superiority of the ANN model over the other applied models in forecasting the maximum UHI intensity was its ability to take complex non-linear interactions into accounts. Also, according to MLR model, the most important input variable was the maximum UHI intensity for the previous day.

The previous publications are different with respect to the types and sizes of the buildings investigated, as well as the types of analyses performed. For ANN models, different structures and learning algorithms were implemented. The choices of influential parameters are mostly limited to two or three. The actual input parameters, for indoor air temperature predictions, were mostly related to weather.

When the regression approach was applied, solar radiation was often excluded. The reasoning for the choice of implemented regression models was not provided, even in model comparison cases. Alternative methods were not studied extensively. The scale of the studies varied between a single rooms in a building to several buildings. Impact factors are easily identifiable by their correlation to semantically related factors in the same context and unknown factors have little effect on predictions. For example, when the study is limited to one house or unit, unknown parameters such as wall insulation, internal heat generation, and neighborhood parameters have a negligible effect on the results. Most researchers who have studied indoor temperature predictions paid extra attention to the training stage and less attention to the validation stage. They did not show the applicability of the model to a larger group of buildings within the scale of study. Despite the efforts of

these studies, there are still modelling issues that have not been analyzed. Consequently, in this thesis, all the discussed statistical models will be used to relate the measured outdoor meteorological variables to indoor dry-bulb temperature. The results are interpreted to find the most applicable models for further predictions that can be extended to the whole city.

2.3 Influential Parameters on Indoor Temperature

There are some parameters that have significant role in UHI formation and intensification; and as a result affect the indoor air temperature. These parameters are extensively discussed in literatures associated with formation of heat island or trapping and storing heat inside the urban canopy. The parameters that are mostly considered are shape and height of the building, view factor, city size, population density, meteorological conditions (wind speed, ambient temperature, cloud cover, relative humidity, and atmospheric pressure), and anthropogenic heat released (Landsberg, 1981; Oke, 1988).

In addition, trees, vegetation and ponds within urban areas, solar radiation and aspect ratio (Mirzaei and Haghighat, 2010), surface albedo, altitude (Giridharan et al., 2007); building occupancy (Porrit et al., 2010); building volume (Priyadarsini et al., 2008); location of indoor temperature measurement (Vandentorren et al., 2006); thermal properties of urban materials, and urban geometry (Gobakis et al., 2011) are identified as the most influential parameters that affect the indoor air temperature. Mirzaei et al. (2010) also considered buildings as the main cause of UHI formation. In the following section some of these parameters are discussed in more details.

2.3.1 Outdoor Dry-bulb Temperature

It is well established that outdoor temperature has significant influence on the indoor environment condition. Oikonomou et al. (2012) suggested that, this should be taken as an important parameter. Also, dry bulb temperature has been measured and considered in many models (Gobakis et al., 2011; Arnfield, 2003).

2.3.2 Solar Radiation

Due to the ability of urban surfaces in trapping radiation and storing heat, solar radiation contributes in formation of diurnal UHI, in equatorial climate, especially when the sky is clear (Bonacquisti et al., 2006; Mirzaei and Haghighat, 2012).

Many urban surfaces such as roadways and buildings' envelopes have low albedo (reflectivity) that absorb a significant amount of incident radiation. Since these low albedo surfaces absorb the heat and release it over the time rather than reflecting it immediately (Giridharam et al., 2007), the absorbed solar energy causes a temperature difference between ambient air and the surfaces, sometimes as high as 50° C (Bardel & Bretz, 1997; Sailor & Dietsch, 2007).

Urban parameters such as sky view factor and built-up or paved area ratio affect the UHI intensity (Park, 1986; Bottyan & Unger, 2003). However, calculating the sky view factor for each surface in addition to the view factor between a surface and other surfaces is one of the problems in radiation modeling (Mirzaei and Haghighat, 2010).

In addition to short wave radiation, surfaces also gain and lose heat through long wave radiation exchange with the environment (Sailor & Dietsch, 2007). The long-wave radiation mostly contributes in formation of nocturnal UHI (Mirzaei and Haghigat, 2010). Therefore, developing a model to calculate the long-wave radiation exchange from each surface to the sky and other surfaces will be important (Chen et al., 2004).

2.3.3 Local Wind Velocity

Velocity field information is necessary to study the effect of flow pattern and formation of atmospheric phenomena, and to calculate the sensible and latent heat fluxes. Lam et al. (2010) stated that buildings increase the roughness of the surface underlying the atmosphere therefore wind speed decreases near the ground. Mirzaei and Haghigat, (2010) suggested to use power law to calculate the local wind speed.

Air movement over the building surface affects the convective heat transfer at the building surface which is an important factor in heat transmission through the building enclosure, surface temperature, and cooling rates. Natural ventilation by means of wind is of considerable importance for cooling during summer when air conditioning is not used (Hutcheon & Handegord, 1983). Wind speed influences the development and intensity of the UHI, suggesting that UHI decreases with increasing wind velocity (Mirzaei and Haghigat, 2010; Kolokotroni et al., 2006).

2.3.4 Relative Humidity

In addition to dry bulb temperature, relative humidity also is considered in many models as one of the influential parameters in formation of UHI (Sailor & Dietsch, 2007; Bonacquisti et al., 2006). Giridharan (2007) mentioned that lack of moisture tends to increase nocturnal UHI.

2.3.5 Location of indoor temperature measurement

Urban settings often include high-rise buildings. Residence of the top floors of such buildings are at a greater risk of overheating, heat related illnesses, and deaths (Barrow and Clark 1998). Mavrogianni et al. (2012) observed a relationship between different floors of the building and their indoor temperature. According to their results, top floor in high-rise structures is in higher risk of overheating compare to the lower floors. Vandentorren et al., (2006) showed that living in the top floor of poorly conditioned dwellings increases the risk of heat illnesses.

2.3.6 Vegetation Ratio

It is obvious that in metropolitan cities, parks have lower temperature compared to high-density areas. In other words, replacing vegetation with built-up areas leads to having warmer temperature in these areas than suburbs (Givoni, 1998; Emmanuel, 1997; Shashua et al., 2006). Schuman (1972) discovered that areas of cities with more concrete and less vegetation exhibited higher mortality rate due to heat-related illnesses.

In principle, increasing vegetation cover decreases the peak summertime urban air temperature (Oke, 1988). Vegetation covers (trees) affect the environment energy balance by transpiration from leaves, reducing the penetration of solar radiation, and blocking the wind (Mochida et al., 2008; Giridharan et al., 2007).

2.3.7 Aspect Ratio (Urban and Building Geometry)

Ambient air temperature within a street canyon depends on the wind speed and velocity profile inside the canyon. Aspect ratio, the ratio of building height to the distance between adjacent buildings, affects the wind velocity profile within a street canyon (Mirzaei and Haghighat, 2010). It has also been shown that the aspect ratio has a negative impact on the cooling rate of the passive and night ventilation (Gobakis et al., 2011).

Bottyan & Unger (2003) considered the height of the building as an effective parameter on UHI. UHI intensity increases with increasing the size of the city and its population (Arnfield, 2003). The areas with compact high rises are warmer compared to parks and low density areas (Bonacquisti et al., 2006).

2.3.8 Occupancy

Another parameter that increases the indoor dry bulb temperature, is the heat generated within the building due to occupancy. Mavrogianni et al. (2012) mentioned the occupation pattern as a key determinant factor of indoor air temperature magnitude. Also, energy consumption by occupants is considered as an influential in many models (Sailor & Dietsch, 2007; Porritt et al., 2010; Bonacquisti et al., 2006).

2.3.9 Time of the day

Gobakis et al. (2011) and Mirzaei et al. (2012) used this parameter in their models. Mirzaei et al. (2012) claimed that integrating the time of the day would improve the performance of the ANN model since some parameters are time dependent (i.e. wind and relative humidity). In fact, it helps the ANN model to distinguish between peak hours and off-peak hours (morning hours) in terms of thermal analysis.

2.3.10 Building Volume

The total building volume is proportional to the building thermal mass. The higher the thermal mass in a building the more energy the building is able to store. Thermal storage of building materials is an important factor in the urban energy balance. It causes reduction in temperature swings (Mirzaei et al., 2012). If misplaced or misused, thermal mass has the potential to increase duration of indoor overheating (Gupta and Gregg, 2012).

The effect of buildings on formation of UHI is not negligible, since buildings change the energy balance in urban areas. Building masses increase the thermal capacity which directly affects the city temperature (Priyadarsini et al., 2008). The heat that is stored during the day in a building creates a temperature difference between urban and rural areas and causes a time delay between the peak temperature of indoor and outdoor (Mirzaei and Haghighat, 2010; Priyadarsini et al., 2008).

2.3.11 Other Factors

From the simulation results, Oikonomou et al. (2012) concluded that shading can affect the indoor temperature. In their study, shading caused a decrease in indoor temperature while in some other cases it had no effect on it. Lack of cross ventilation for single facing buildings is mentioned as a factor that increases the indoor temperature more compared to double facing buildings (cross ventilation).

Building age, type, and insulation level were considered important determinant factors on indoor thermal conditions (Mavrogianni et al., 2012). In addition, anthropogenic heat release is considered as another main cause in formation of UHI especially in high rise and dense metropolitan areas (Mirzaei and Haghighat, 2010).

The above literature review indicates that data analyses for indoor air temperature prediction were focused on the relationship between the indoor and outdoor conditions, relying mainly on outdoor air temperature. Hence there is a need to provide a method for indoor temperature prediction by studying outdoor thermal conditions, building characteristics, and building environmental surrounding factors. In the methodology section, the implementation of the parameters affecting the indoor temperature is discussed.

Chapter 3

Measurements

3.1 Measurements and Localization

In general, UHI effects can be measured directly and/or indirectly. For the direct measurement method, sensors are used at fix or mobile observation stations to measure the surface or air temperature. For the indirect method, satellite and/or airborne images are used. Based on the method and scale of measurements, different approaches can be used to study the UHI phenomena (Health Canada, 2011). A comprehensive field measurement activity was conducted in the Montreal Island (Park et al., 2010). The result of the field measurement study in Montreal is used in this study for the development of the models. A brief description of the study area, measurement techniques, etc. is given in this chapter.

3.2 Study Area

The field measurement study was carried out in the city of Montreal, Canada, with a population listed as slightly fewer than 4 million (Canada Census, 2011). Winters in Montreal are often cold, snowy and windy. Most days stay near or below freezing ($+2^{\circ}$ to -8°C), with well below freezing at night (-10 to -15°C). Wind chill during the winter in Montreal is an important factor to be considered. The average annual snowfall in Montreal is approximately 2.1 meters. Summers in Montreal are warm, hot and humid. Average daytime temperature stays between 24°C to 28°C and overnight temperature is around 16°C . However, on many days temperature reaches and even exceeds 30°C , which combined with high level humidity it is felt much hotter. July and August are the warmest

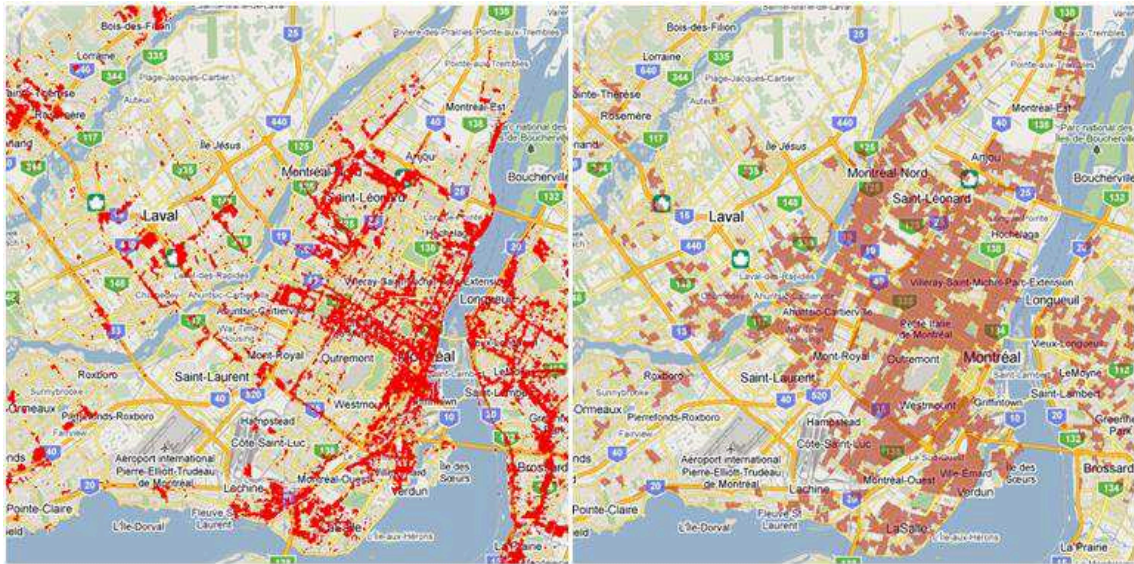
months in Montreal and throughout Canada (National Climate Data and Information Archive, 2012; World Guides, 2013). The housing insulation mostly designed for cold weather than summertime heat. It is noteworthy to mention that cities which experience large seasonal temperature range are more vulnerable to heat related mortality (Tan et al., 2004).

3.3 Data

Meteorological data were obtained from the weather station (Pierre-Elliot Trudeau airport). Four variables were measured hourly including outdoor dry-bulb temperature, wind speed, solar radiation, and relative humidity. In order to identify the vulnerable regions, first, satellite thermal images were utilized to characterize Montreal urban areas and zones with high surface temperature in summer. Then, ‘Urban Heat Island Mapping Tool’ was used to evaluate and choose potential zones for recruiting potential buildings. This tool made it possible to locate the most exposed areas to UHI in Montreal Island by considering four additional influential factors:

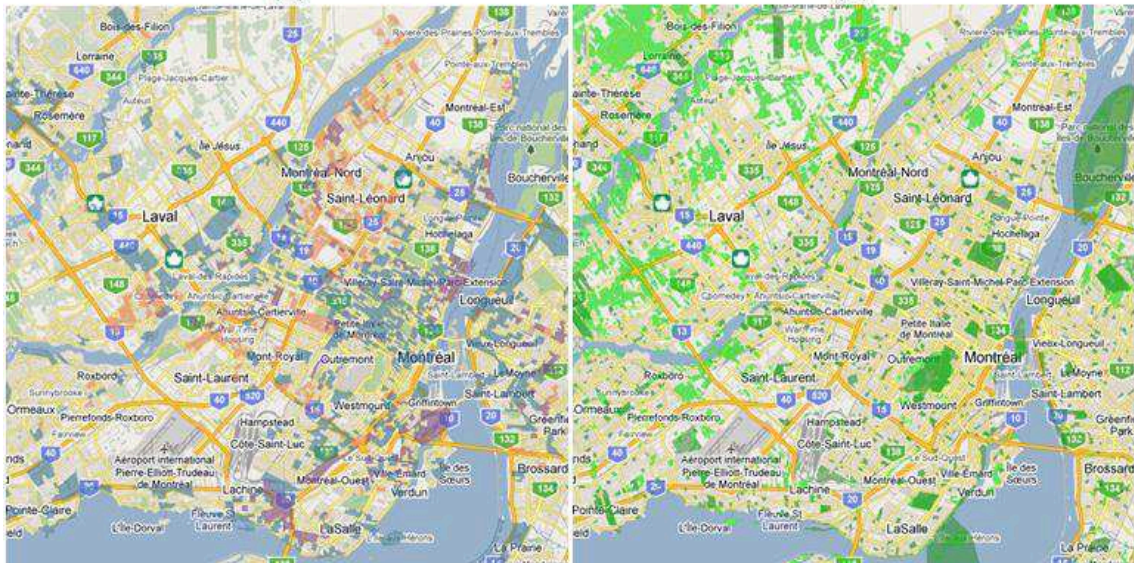
- a. areas determined to have the highest surface temperatures with a minimum density of 400 inhabitants per km² (Figure 3.1 (a)),
- b. areas with population density more than 5001 people per km² (Figure 3.1 (b)),
- c. areas included deprived occupants who cannot afford air conditioning (Figure 3.1 (c)), and
- d. Areas located far from vegetation or with low vegetation ratio (Figure 3.1 (d)) (Park et al., 2010).

Finally, 55 residential buildings in ten zones were identified on the Island of Montreal shown in figure 3.2. Building locations are listed in Table 3.1. A measurement campaign was conducted to monitor the indoor thermal characteristics of these 55 residential buildings in most vulnerable regions in the Montreal Island (Park et al., 2010). About sixty five percent of recruited building types were duplex and triplex; most typical of residential buildings on the Island of Montreal.



(a)

(b)



(c)

(d)

Figure 3.1 (a) High surface temperatures, (b) high population density, (c) socio-economically deprived areas, and (d) minimal vegetation.

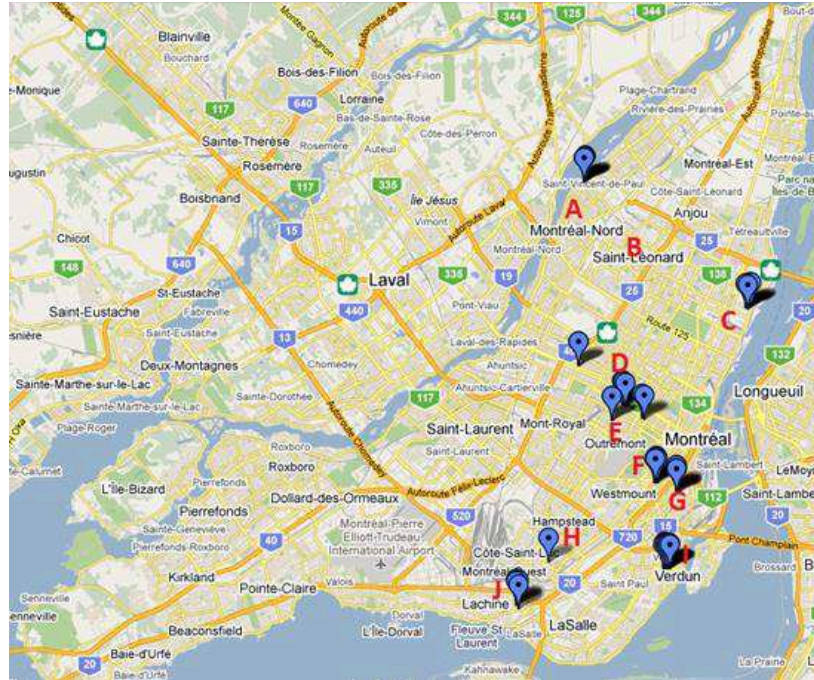


Figure 3.2 Location of buildings under study

Table 3.1 Regions under study on the Island of Montreal

Zone	Name	Number of Buildings
A	Montréal-Nord	6
B	Saint-Léonard	2
C	Mercier Hochelaga-Maisonneuve	5
D	Le Plateau-Mont-Royal	7
E	Outremont	2
F	Ville-Marie	7
G	Le Sud-Ouest	5
H	Côte-des-Neiges Notre-Dame-de-Grace	1
I	Verdun	16
J	Lachine	4

Further details about the measurement campaign and instrumentation can be found in the report (Park et al., 2010).

According to the measurement campaign, the location for installing an indoor sensor was selected using a variety of criteria. These locations were selected to be close to the thermostat and away from windows or other ventilation sources. They should not be influenced by solar radiation or temperature fluctuations caused by air movement. Indoor air temperature and relative humidity were recorded at a ten minutes interval. The collected 10-minutes intervals raw data were averaged into hourly data for analyses.

Figure 3.3 shows hourly maximum and minimum indoor air temperatures measured in the 55 dwellings along with the corresponding outdoor air hourly temperature for the period of heat wave occurred during July 5th to July 8th, 2010. Figure 3.4 represents the same information for the second heat wave occurred during August 30th to September 3rd, 2010. It is clear that maximum and minimum indoor air temperatures are greater than their corresponding outdoor air temperatures during the periods of occurrence of heat waves.

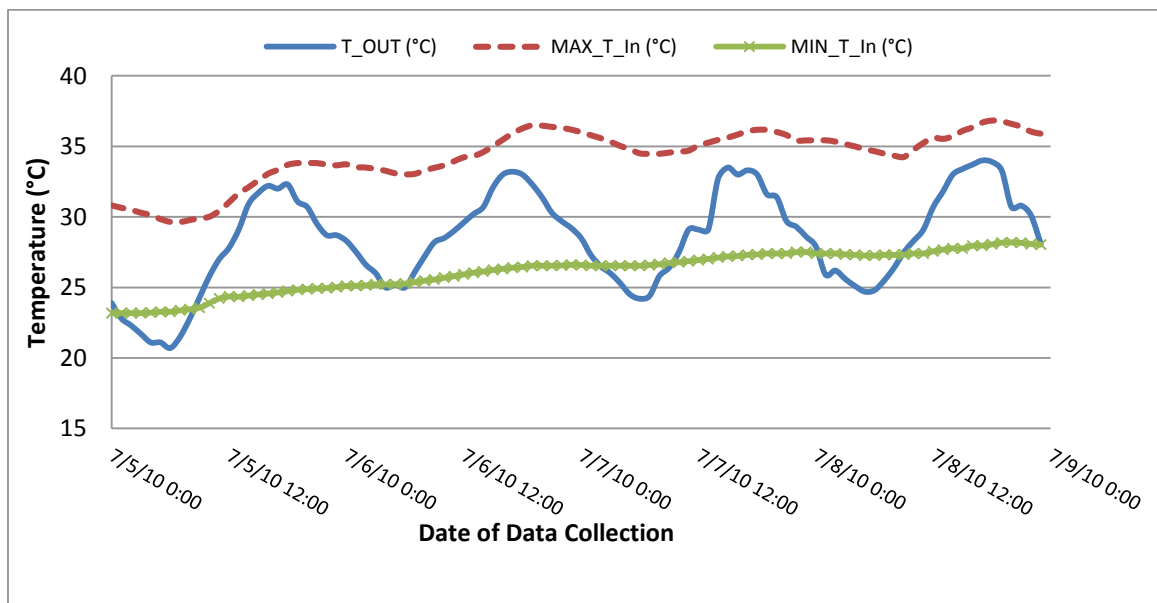


Figure 3.3 Hourly maximum and minimum indoor thermal conditions during first heat wave (July 5th to July 8th, 2010)

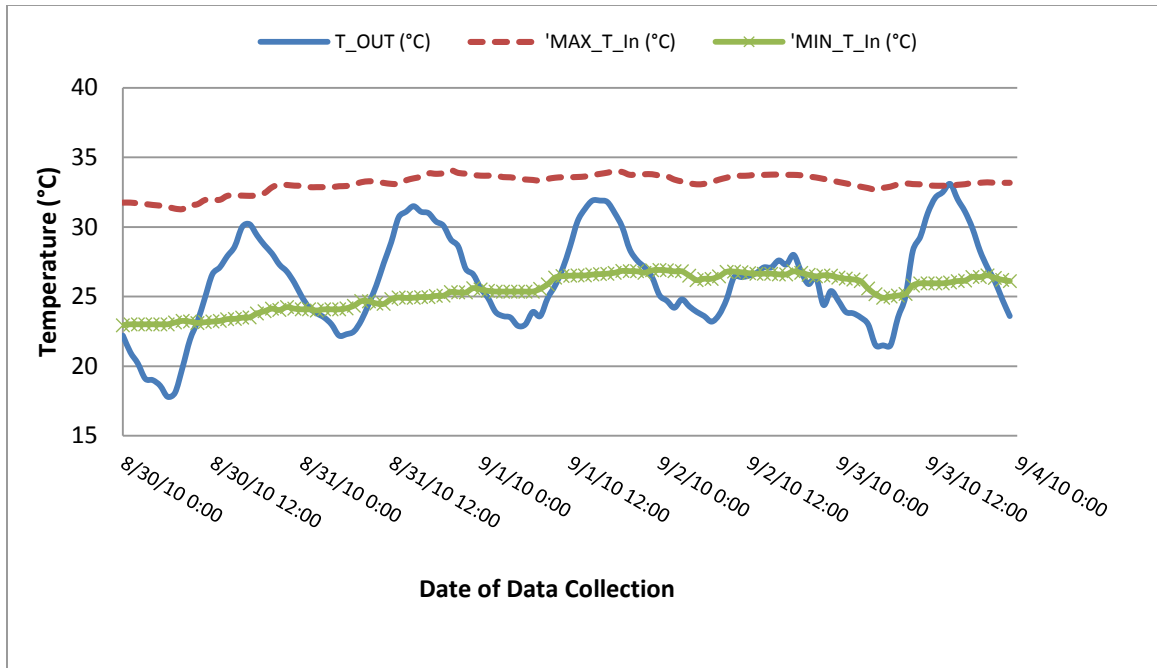


Figure 3.4 Hourly maximum and minimum indoor thermal conditions during second heat wave (August 30th to September 3rd, 2010)

Figure 3.5 shows hourly indoor dry-bulb temperature measured in two different units along with the corresponding hourly outdoor dry-bulb temperature for the first twenty days of July 2010. Both units (BLDG9 & BLDG10) are located in the same building: BLDG9 is located on the top floor of the building. It is clear that the top floor unit is always warmer around 5 °C than the other unit. In addition to corresponding indoor air temperature of BLDG9 and BLDG10, measured data related to outdoor weather conditions for the first day of June 2010 are presented in Table 3.2 as a sample of whole dataset that was used in this study.

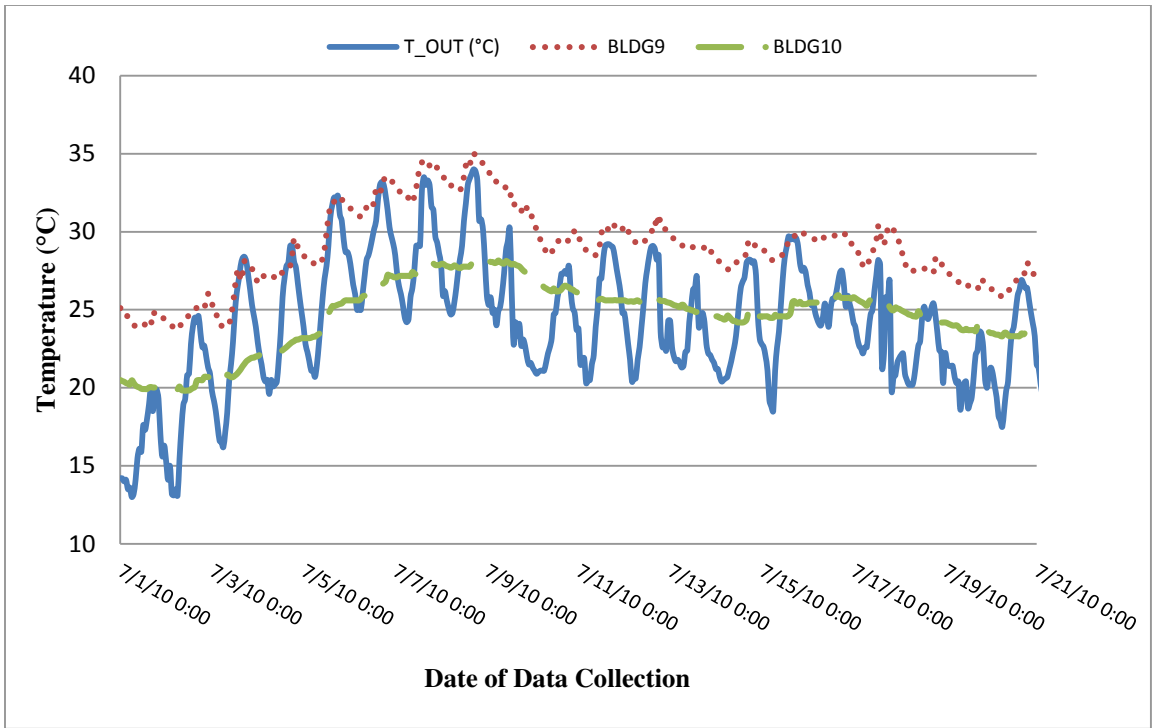


Figure 3.5 Hourly indoor dry-bulb temperatures of BLDG9 & BLDG10 during July 1st to July 20th

Table 3.2 Sample measured data

Date-Time	Temperature (°C)			Wind Speed (km/h)	Solar radiation (W/m ²)	Relative Humidity (%)
	Outside	BLDG9	BLDG10			
6/1/10 0:00	14.2	25.1	20.5	4	0	56.0
6/1/10 1:00	14.2	25.1	20.4	4	0	51.0
6/1/10 2:00	14	24.9	20.4	17	0	53
6/1/10 3:00	14.1	24.7	20.3	17	0	55
6/1/10 4:00	13.5	24.5	20.3	13	0	61
6/1/10 5:00	13.6	24.3	20.2	17	0	61
6/1/10 6:00	13	24.1	20.5	9	5	61
6/1/10 7:00	13.2	24.0	20.3	9	21	67
6/1/10 8:00	14.1	23.9	20.1	4	91	88
6/1/10 9:00	15.5	23.9	20.1	11	73	91
6/1/10 10:00	16.1	23.8	20.0	11	262	93
6/1/10 11:00	15.9	23.9	19.9	17	54	94
6/1/10 12:00	17.6	23.9	19.9	6	153	95
6/1/10 13:00	17.3	24.1	19.9	11	184	92
6/1/10 14:00	18	23.9	19.9	6	419	90
6/1/10 15:00	18.9	23.8	20.0	6	606	85
6/1/10 16:00	19.9	24.0	20.0	4	601	77
6/1/10 17:00	18.5	24.8	20.0	15	434	81
6/1/10 18:00	19.8	24.8	20.0	13	251	77
6/1/10 19:00	19.9	24.8	20.0	17	98	76
6/1/10 20:00	19.3	24.7	20.0	17	2	80
6/1/10 21:00	17	24.6	19.9	15	0	81
6/1/10 22:00	15.6	24.5	20.0	15	0	82
6/1/10 23:00	16.3	24.4	19.9	13	0	85

Chapter 4

Methodology

4.1 Model Validation Criteria

As it is mentioned in the introduction, the indoor thermal environment and in particular overheating effects are complex phenomena with multiple correlated factors. However, limited research has been conducted to date to predict indoor air temperature with regards to the weather factors and neighborhood parameters. To achieve this in the present study, statistical models were adopted as they require lower computational time compared to analytical models.

In this study, root mean square error (RMSE) is used as the goodness of fit to evaluate the prediction accuracy of the proposed model. It is defined as:

$$RMSE = \left[\frac{1}{m} \sum_{i=1}^m (\hat{Y}_i - Y_i)^2 \right]^{1/2} \quad (2)$$

where \hat{Y} is the predicted output and Y is the measured one and m is the number of observations.

4.2 Input Data and Variables

Hourly measured meteorological parameters (outdoor dry-bulb temperature, relative humidity, direct normal solar radiation, and wind velocity) are used as input variables for statistical models. Measured indoor dry-bulb temperature is the output of the

models. The goal is to develop models to predict the indoor temperature during heat waves in Montreal.

In order to take into consideration the effect of building envelope characteristics (Albedo and thermal capacity), the location of living area, and the outdoor environmental conditions around the buildings (neighborhood), the studied buildings are divided into four groups:

- a. Top floor dwellings located in downtown Montreal.
- b. Other dwellings located in downtown Montreal.
- c. Top floor dwellings located in other sample areas.
- d. Other dwellings located in other sample areas.

For this purpose, downtown Montreal was approximately assumed bounded by Sherbrooke Street to the north, Papineau Avenue to the east, Atwater Avenue to the west, and the Ville-Marie Expressway to the south. By considering this segmentation, 12 buildings out of 55 are located in the downtown area.

4.2.1 Building Height

The heights of most buildings located in the downtown are around 20 m to 30 m. Only three of the buildings in the downtown do not have the same height (around 10 m). These three buildings can represent other residential buildings in downtown at a height of around 10 meters. The remaining buildings are below the height of ten meters except two of them that are located on Jarry Street with heights of around 17 meters.

4.2.2 Wind Effect

Generally, wind speed measurements are taken at the meteorological stations. In this study, it is important to consider the impact of urban canyon on the wind speed. Therefore the weather data collected at the meteorological station must be modified in order to reflect the canyon boundary layer effect. This was done using the power law to take into account the effects of surface roughness and height above ground (Hutcheon & Handegord, 1983):

$$\frac{v_z}{v_g} = \left[\frac{z}{z_g} \right]^\alpha \quad (3)$$

where Z is the height of the buildings under study. The mean speed exponent (α) corresponds to the terrain category over which the under studied buildings and the airport are located. V_z is the mean speed at specified height. V_g and the Z_g are the gradient speed and gradient height, respectively.

Two different wind speed profiles were considered for Montreal Island. One of them represents the wind speed in downtown, and the other one represents the wind speed for other sample areas under study. It was assumed that Pierre-Elliot Trudeau International Airport is located in terrain category number 3 in Montreal Island. The average height of the studied buildings in the downtown Montreal was 25 m. For the rest of Montreal, the average height of these buildings was 8 m. In order to calculate the wind speed in downtown Montreal both terrain and height changes were considered. But, for other sample areas only height difference was taken into consideration since it is assumed these areas have a similar terrain category as the airport.

4.2.3 Aspect Ratio

Aspect ratio, as explained in section 2.3.7, is the ratio of the building height to the distance between adjacent buildings. Aspect ratios of buildings in downtown vary from 0.95 to 1.6, and it is around 0.5 for the three buildings in downtown with lower heights of around 10 m. The buildings located outside the downtown have lower aspect ratio values, which vary from 0.18 to 0.39. For those two exceptions with higher heights (around 17 meters) outside the downtown, it is around 0.54.

4.2.4 Building Volume and Occupancy

Buildings which are located in downtown Montreal have greater volumes compared to the rest of the studied buildings. It is roughly estimated that building volumes vary from 12000 m³ to 29000 m³ in downtown. This value is just under 5000 m³ for the rest of the buildings. It is obvious that buildings with greater volume have greater exposed surface areas and greater internal heat generation (Mirzaei et al., 2012).

It is important to note that the number of occupants in all dwellings is almost constant since most of the studied buildings contain small units. Based on the measurement campaign, the number of occupants in 80% of dwellings was less than three people. Therefore, greater internal heat generation in downtown buildings relates to the greater number of units in those buildings.

4.2.5 Vegetation and Albedo

By studying images acquired from Google Maps, Satellite view mode, it can be concluded that downtown Montreal has the lowest vegetation ratio among sample areas. Roof albedo and envelope albedo of all studied buildings were considered to be 0.15 and 0.25, respectively.

4.2.6 Sensor Location

The sensor location refers to the ratio of a building floor in which the temperature sensor was located to measure the indoor temperature to the total number of floors in the building. By this definition sensor location varies between zero and one. It is an important parameter for indoor temperature prediction. As discussed before, the top unit (dwelling) of any building has the worst indoor thermal conditions. In order to highlight the effect of sensor location, the buildings in which measurements took place in their top floor are studied separately. This segmentation helps to study the effect of solar heat gain in top floor units and other floors of the buildings separately.

4.2.7 Solar Heat Gain

The purpose of the solar radiation model is to estimate the hourly heat gain by building enclosure due to direct normal radiation as well as total diffuse radiation. It is assumed that the heat gain is isotropic. The model uses a series of measured data gathered by measurement campaign and some calculations in order to obtain the heat gain. First, direct normal solar radiation data was collected on an hourly basis throughout the months

of June, July, and August 2010 at Pierre-Elliot Trudeau International Airport. Then, the total diffuse radiation on vertical surfaces, I_d , was calculated (Hutcheon & Handegord, 1983):

$$I_d = I_{DN} \times [C \times F_{ss} + 0.5\rho_g(C + \sin\beta)] \quad (4)$$

I_d is a function of the direct normal solar radiation, I_{DN} , the diffuse radiation factor, C , the angle factor between vertical surface and the sky, F_{ss} , the ground reflectance, ρ_g , and the solar altitude angle, β . The diffuse radiation factor of 0.134, 0.136 and 0.122 are used for the months of June, July and August, respectively. Also, an estimated value of 0.2 for ground reflectance was used. In addition, hourly solar altitude angles were calculated for the mentioned months, taking into account the transformation of local standard times to the apparent solar.

Lastly, in this model, all building surfaces including the roof, the exterior walls, and the windows were taken into account to estimate the building heat gain. The construction materials for the latter were also considered in order to determine their albedo and transmittance. Building dimensions are required to calculate the appropriate surface areas. The number of windows and their surface areas are also needed. The total hourly heat gain due to solar radiation is then proportional to:

$$\text{Heat Gain} = A_{Wind} \times I_d \times \tau_{wind} + A_{roof} \times I_{DN} \times (1 - Albedo_{roof}) + A_{env} \times I_d \times (1 - Albedo_{env}) \quad (5)$$

where A_{Wind} , A_{roof} , and A_{env} represents surface area (m^2) for windows, roof and walls, respectively, and τ is the window transmittance that was assumed 0.85. The above formula

generates the actual heat gain value for any building. But it cannot be used directly in this thesis since a group of buildings should be modeled. Further assumptions and calculations has been made as follow.

The solar heat gain per area of each building assembly (roof, wall, and window) was calculated. It is a function of the solar time, material properties for different assemblies, as well as inclination angle of that surface with respect to horizontal plane and facing orientation of that assembly. Based on the total heat gain per area of assemblies, the percentage gains of direct normal solar radiation on the building by every assembly were calculated. These values are almost constant for each assembly regardless of the location of the building. In case of top floor units, by considering both horizontal and vertical surfaces, it was calculated that about 65% of direct normal solar radiation is absorbed by assemblies. For the rest floors of the sample study, this value was calculated about 14%.

4.2.8 Sol-air Temperature

The sol-air temperature is defined as the outside air temperature which, in the absence of solar radiation, would give the same temperature distribution and rate of heat transfer through the walls and roof due to the combined effects of the actual outdoor temperature distribution and the incident solar radiation (Tham & Muneer, 2011). In this study, the sol-air temperature is used to take the combined effect of solar radiation and outdoor ambient temperatures into consideration at the same time. The regression methods that were used in this study were not able to accurately combine the effect of solar radiation and outdoor dry-bulb temperature. In other words, the frequencies of appearance of zero values for solar radiation and their differences with other non-zero values make the

regression models unable to accurately predict the temperature. The sol-air temperature concept employed to avoid this problem. Moreover, using sol-air temperature reduces the number of input variables for each method which simplifies the analysis. The following formula represents the sol-air temperature:

$$T_e = T_o + \frac{\alpha I_t}{h_o} - \frac{\epsilon \Delta R}{h_o} \quad (6)$$

where T_e is the sol-air temperature and h_o is the assigned surface conductance. The combined coefficient h_o is equal to the sum of the convection and radiation coefficients. The value of h_o is subjected to substantial variation with both temperature and wind speed over the surface, but a value of 23 W/ (m². °C) is commonly used. The value of the emittance, ϵ , is commonly taken as 1. An approximate value of ΔR for horizontal surfaces is about 60 W/m². For vertical surfaces it is commonly assumed that $\Delta R = 0$ (Hutcheon & Handegord, 1983). The values of absorptance, α , for solar radiation were discussed above for different types of building under studied.

4.3 Input Data Processing

In previous section (section 4.2), four different unit groups were defined: a) top floor units of the dwellings located in downtown of Montreal, b) other floors' units of the dwellings located in downtown of Montreal, c) top floor units of the dwellings located in other zones; and d) other floors' units of the dwellings located in other zones. In order to find the worst case scenario which is the target of this study, the above information and assumptions are summarized in the table 4.1 to make these comparisons easier.

Table 4.1 Characteristics of under studied buildings

Segmentation	Height (m)	Aspect Ratio	Occupancy (Occupant / m ²)	Volume (m ³)	Vegetation Ratio	Roof Albedo	Envelop Albedo	Sensor Location
DT - Top (a)	20 ~ 30	0.95 ~ 1.6	same	12k ~ 29K	Low	0.15	0.25	1
DT - Other (b)	20 ~ 30	0.95 ~ 1.6	same	12k ~ 29K	Low	0.15	0.25	(0, 1)
Other - Top (c)	< 10	0.18 ~ 0.39	same	< 5k	High	0.15	0.25	1
Othe - Other (d)	< 10	0.18 ~ 0.39	same	< 5k	High	0.15	0.25	(0, 1)

All the variables mentioned in Table 4.1 for categories (a) and (b) in downtown Montreal have the same value except for the location of sensor. This number (sensor location) is one for the top units. The exposed surface area of the façade is larger in those units. Therefore, the amount of solar radiation that a top unit gains is larger. As discussed in section 4.2.7, top floor units absorb around 65% of incident solar radiation. This value reduces to 14% for other floors. Therefore, by assuming that other influential parameters for dwellings located in downtown Montreal are constant, it is reasonable to consider the top floor units as the target study in this area. Following the same reasoning for the dwellings located in other sample areas (categories (c) and (d)), it can be concluded that in those areas again the top floor units have the worst thermal condition. So they can be considered as the target study in those areas as well.

To find the worst case scenario for heat waves between categories (a) and (c), their related influential parameters were compared together. Both categories have the same values for occupancy, roof and envelop albedo, and sensor location. By assuming that overshadowing does not happen in top floors, it can be concluded that all top floors receive the same amount of solar radiation per unit area. Aspect ratio affects shading by buildings as well as wind speed in the street canyons.

The building volume, which represents the building thermal mass, is greater for buildings that are located in downtown Montreal. The building volume can trap the heat. The vegetation ratio is lower in downtown area compared to other studied areas. Height and the location of the buildings affect the wind speed and as a result indoor air temperature in top floors. The wind speed calculated in downtown (category (a)) is lower than those in category(c). Figure 4.1 illustrates a sample of wind speed measured at the airport along with the corresponding wind speed values for downtown (categories (a)) and other sample areas (categories (c)). It can be seen that buildings that belong to category (a) are exposed to the lowest wind speed.

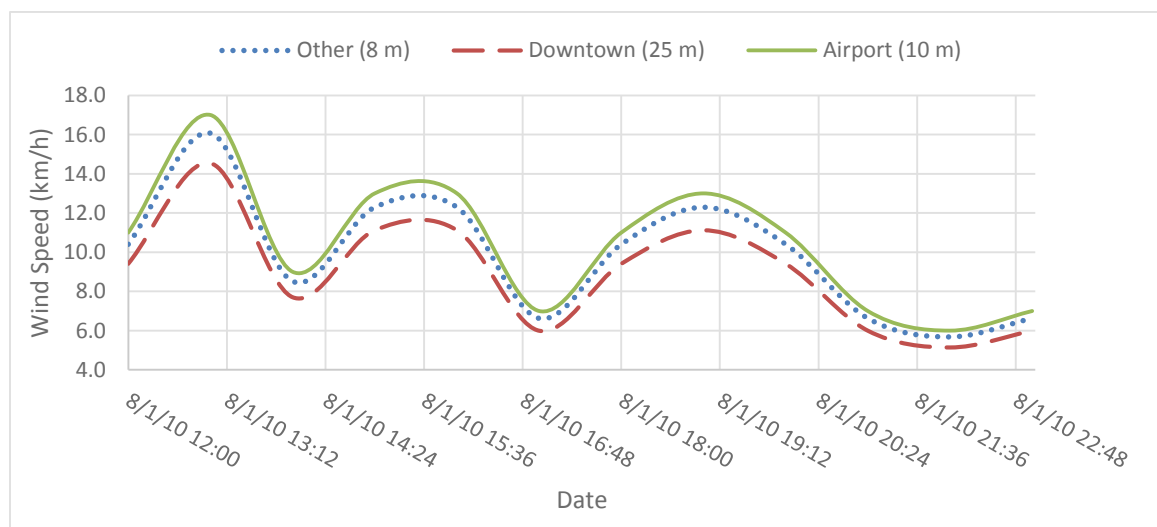


Figure 4.1 Wind speed at airport, downtown, and other sample areas of study

It can be concluded that the top floor units in the dwellings that are located in downtown Montreal have the worst indoor thermal condition during the heat waves and should be chosen as the target of this study.

This conclusion is supported by results of the indoor dry-bulb temperatures accumulated by the measurement campaign. Measured indoor dry-bulb temperatures

related to top floor dwellings in categories (a) and (c) shows that top floor dwellings that are located in downtown have the worst indoor thermal condition during the heat waves. Figures 4.2 and 4.3 show measured indoor dry-bulb temperature of one building in downtown (category (a)) and two midrise buildings in category (c) for the period July 3rd to July 10th, 2010. Note that a heat wave occurred during July 5th to July 8th, 2010.

Any increase in the height of the building will result in an increment in total heat capacity of the building. To compare the effects of height and location on the indoor air temperature two different cases were proposed.

In Figure 4.2, dwelling no. 28 (BLDG28) is located on the top floor of a high rise building in downtown Montreal. As it is shown, during the heat wave, indoor dry-bulb temperatures of those buildings are very close and follow the same trend. They even have the same peak values in some instances. BLDG 28 has greater volume and thermal mass in comparison with the other two sample buildings. Therefore it takes more time for BLDG 28 to reach its peak value. Higher thermal mass due to higher height of the building results in more heat absorption. By the end of the heat wave, the temperature drop in BLDG28 is more gradual compared to the other two buildings. In addition, its indoor thermal fluctuations are less than other sample buildings.

In Figure 4.3, the height and volume of selected buildings are almost identical. The height and volume of these three buildings are around 8 m and 1000 m³, respectively. Building no. 25 (BLDG25) is located in downtown Montreal. Figure 4.3 shows that during, before, and after the heat wave, its hourly measured dry-bulb temperature is significantly greater than those of other two sample buildings. Also, their temperatures fluctuations are

similar to each other. Moreover, they follow the same trend during the temperature increase and decrease, and reach their peak values at almost the same time.

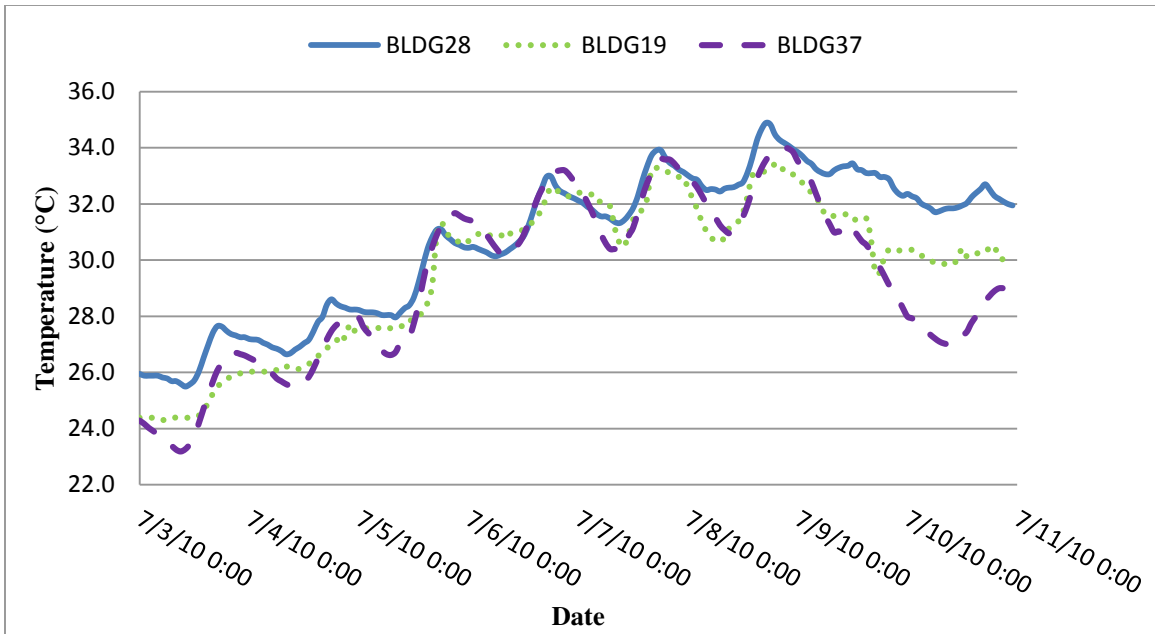


Figure 4.2 Measured indoor dry-bulb temperature for buildings no. 28, 19, 37 (BLDG28, BLDG19, BLDG37)

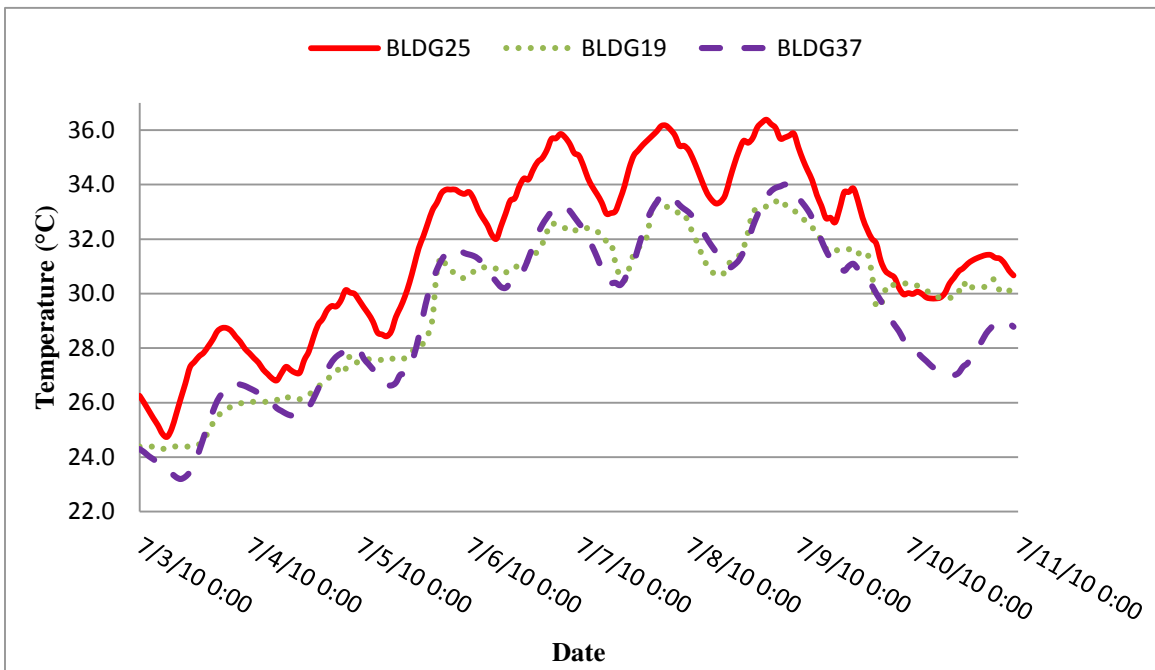


Figure 4.3 Measured indoor dry-bulb temperature for buildings no. 25, 19, 37 (BLDG25, BLDG19, BLDG37)

4.3.1 Linear Regression

The objective of the linear regression (LR) analysis is to study the relationship between one independent variable and one dependent variable. The assumption of the model is that the relationship between the dependent variable Y and the independent variable X is linear. In other words, this method fits a straight line through the set of points of observation in such a way that makes the sum of square residuals of the model minimum. The following represents a LR model:

$$Y = aX + b \tag{7}$$

a and b are fitting coefficients.

4.3.2 Multiple Linear Regressions (MLR)

In many problems, two or more independent variables are related to one dependent variable. The objective of MLR method is to explore the relationship between independents, predictors, or repressor variables and a dependent or criterion variable while it is assumed that the relationship between dependent variables and independent variable is linear. The following is called a MLR equation (ASHRAE Fundamentals, 2009).

$$Y = \beta_0 + \beta_1 X_1 + \beta_2 X_2 + \dots + \beta_k X_k \tag{8}$$

where β_s are the coefficients, and k is the number of observations. The method of least squares is typically used to estimate the regression coefficients in a MLR model so that the sum of the squares of the errors, is minimized. Once one set of observed data points was used to find the coefficients, the model can be used to predict dependent variable based on

new set of independent variables. This model describes a hyper plane in the k-dimensional space of the independent variables.

4.3.3 Time Series

In statistics, time series analysis is the study of data collected in a certain period of time to determine an outcome in relation to its history. All these data are taken at different times, but spaced in the same time interval. Time series analysis comprises methods for analyzing time series data in order to extract meaningful statistics. In fact, time series forecasting is the use of a model to predict future values based on previously observed values. To achieve these results, it is important to make an analysis of the phenomenon by evaluating the data collected. Finally, an assumption about the final outcome of the experiment should be taken into consideration.

This method was popularized by its usefulness as a tool of choice for evaluating the prediction of future results (Gardner 2006; Muth 1960). There are several types of data analysis available for time series which are appropriate for different purposes. The results of empirical research by Makridakis et al. (1983) have proven that simple exponential smoothing is the best choice for time series forecasting, from among 24 other time series methods that often produce quite accurate forecasts. The autoregressive model is one of a group of linear prediction formulas that attempt to predict an output of a system based on the previous inputs. The following represents a simple exponential smoothing time series equation which is well known as autoregressive model (AR) and was used in this study:

$$T_i(t) = \alpha_0 + \alpha_1 T_e(t) + \alpha_2 T_e(t - 1) + \dots + \alpha_p T_e(t - p) + \beta W(t) + \gamma RH(t) \quad (9)$$

where α_i and β are the coefficients. $T_i(t)$ is the indoor dry-bulb temperature measured at time t . $T_e(t)$ represents the sol-air temperature calculated at time t , based on the outdoor dry-bulb temperature and direct normal solar radiation. $RH(t)$ is the relative humidity. $W(t)$ represents the wind speed.

4.3.4 Multiple Non-Linear Regression (MNLR)

It is assumed that the relationship between dependent variable and independent variables is non-linear in multiple non-linear regression models. The following is called a MNLR equation (Adamowski et al., 2012).

$$Y = \beta_0 + \beta_1 X_i + \beta_2 X_j + \beta_3 X_k + \beta_4 X_i^2 + \beta_5 X_j^2 + \beta_6 X_k^2 + \dots + \beta_p X_i X_j X_k \quad (10)$$

where β_0 is the intercept, β is the coefficient, and p is the number of observations. The method of least squares is typically used to estimate the regression coefficients in a MNLR model so that the sum of the squares of the errors is minimized. Once one set of observed data points was used to find the coefficients, the model can be used to predict dependent variable based on new set of independent variables.

The MNLR model may often still be analyzed by MLR techniques (Montgomery 2008). For example consider the following second-order MNLR model in two variables:

$$Y = \beta_0 + \beta_1 X_1 + \beta_2 X_2 + \beta_3 X_1^2 + \beta_4 X_2^2 + \beta_5 X_1 X_2 \quad (11)$$

If let $X_3 = X_1^2, X_4 = X_2^2, X_5 = X_1X_2$, then this becomes

$$Y = \beta_0 + \beta_1X_1 + \beta_2X_2 + \beta_3X_3 + \beta_4X_4 + \beta_5X_5 \quad (12)$$

which is a MLR method.

4.3.5 Artificial Neural Network (ANN)

Artificial Neural Network (ANN) is a data-driven process since the analysis and the results depend on the available data. It has the ability of approximation arbitrary and complex non-linear relationship between the large input and output datasets whose analytical forms are difficult or impossible to be obtained. This technique has been used in many research areas such as spectroscopic signal measurement, forecasting future values of possibly noisy multivariate time series based on past histories, and parallel distributed processing (Adamowski et al., 2012; Liu et al., 2006; Kolokotroni et al., 2006).

In this study, the three-layer feed-forward neural network approach was chosen. The selection of layer number of a neural network is the first and crucial step that affects training, validation as well as testing and statistical analysis of the model. It was proved that a three-layer feed-forward neural network can approximate any function when a sufficient number of hidden neurons are provided (Irie and Miyaki., 1998). Also the results performed in the study which was done by Mirzaei et al. 2012, indicate that a three-layer food-forward neural network can adequately model the system.

The second step is to identify the variables. The input layer of the network consists of four neurons. These neurons correspond to sol-air temperature, relative humidity, time

of the day, and neighboring wind speed at Pierre-Elliot Trudeau airport. The output layer which consists of one neuron is the desired target that network should predict (indoor dry-bulb temperature). The goal of neural network is to minimize error functions between prediction and target datasets by adjusting weights and biases.

After the identification of input and output variables, the selection of the size of hidden units becomes crucial for the performance of a neural network. There is no exact rule about how to define the size of hidden units, but still some articles suggest the maximum number of elements in the hidden layer to be twice the input layer dimension plus one (Lu and Viljanen, 2009). In this study, all the possible numbers of hidden neurons were examined to find the most accurate networks. The artificial neural network models are generated using the MATLAB Neural Network Fitting Tool (NNFT) (MATLAB, 2012). Figure 4.4 shows the structure of the feed-forward neural networks used in this study.

To obtain the most practical model for indoor dwelling temperatures prediction that can be attributed to the whole city, all of the above discussed methods were used. But these methods were implemented by a new rearrangement. In fact, linear regression, multiple linear regression, and time series methods are quite similar regression methods. So instead of applying these three methods in this study, time series method was used which represents the other two methods and also takes the effect of thermal mass of buildings into account. Therefore, in this study, Artificial Neural Networks, and Time Series were implemented to predict indoor dry-bulb temperatures of dwelling in Montreal Island.

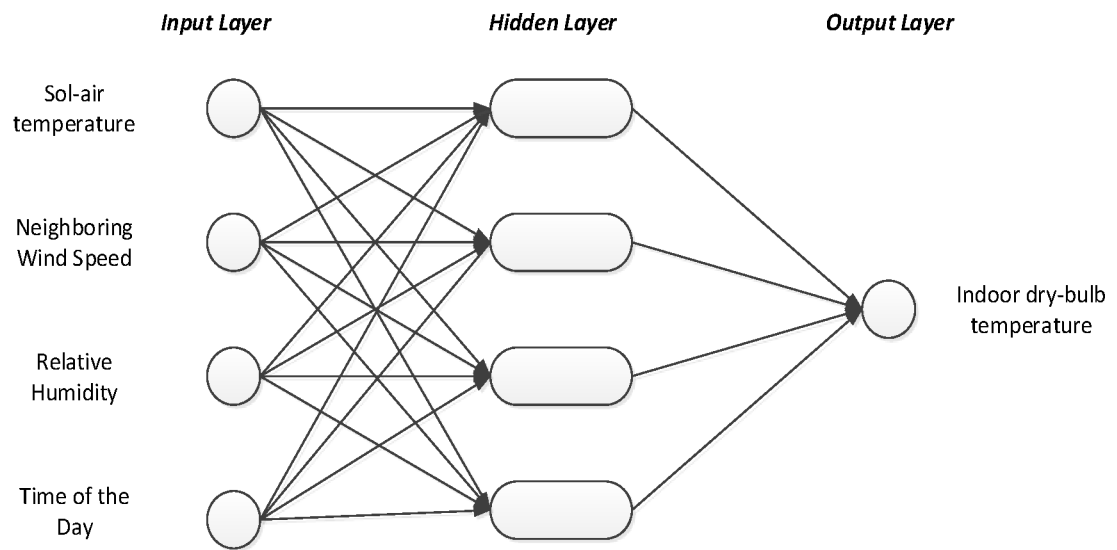


Figure 4.4 Basic structure of 3-layer feed forward neural network with multiple inputs and a single output

Chapter 5

Analysis, Results, and Discussion

5.1 Time Series

5.1.1 Apply the method

The time series model was developed using Analysis ToolPak of Microsoft Excel (2013). The datasets of three units (Building 25, Building 28, and Building 29) which are located in zone (a) corresponding to months June, July, and August 2010 were used to develop the model. The total number of the input and output layer datasets is 6,552.

At the beginning, the input of the model was selected as sol-air temperature ($^{\circ}\text{C}$), wind speed (Km/h), and outdoor relative humidity (%). The indoor dry-bulb temperatures of the selected units were considered as the output. The input variables were then increased gradually by adding sol-air temperature of previous hours (up to 16 hours) to find the best model. The results were getting better by adding more sol-air temperature related to previous hours. After a specific number of input variables no further improvement was observed. To evaluate the model performance, the root mean square error (RMSE) between predicted and actual indoor dry-bulb temperatures was used.

Finally, the best results were obtained by implementing the past 8 hours observed value of sol-air temperatures (totally 11 inputs). The RMSE of the best model is 2.10°C . Also, 77 % and 86 % of the predicted indoor dry-bulb temperatures by this model have an error less than $\pm 2^{\circ}\text{C}$ and $\pm 3^{\circ}\text{C}$, respectively. The RMSE for models including sol-air temperature of zero, four, seven, nine, and ten hours of past time are 2.5°C , 2.29°C , 2.14

°C, 2.12 °C, and 2.16 °C, respectively. The following is the obtained equation for this model:

$$T_i(t) = 16.9 + 0.054 T_e(t) + 0.018 T_e(t - 1) + 0.018 T_e(t - 2) + 0.009 T_e(t - 3) + 0.006 T_e(t - 4) + 0.007 T_e(t - 5) + 0.005 T_e(t - 6) - 0.015 T_e(t - 7) + 0.9 T_e(t - 8) - 0.063 W(t) + 0.073 RH(t) \quad (13)$$

where $T_i(t)$ is the indoor dry-bulb temperature measured at time t . $T_e(t)$ represents the solar air temperature calculated at time t , based on the outdoor dry-bulb temperature and direct normal solar radiation, $RH(t)$ is the relative humidity, and $W(t)$ is the wind speed.

5.1.2 Level 1 Simulation

Once all models were developed and their best fit line was found, they were used to simulate hourly indoor dry-bulb temperatures of units in zone (a). The goal is to determine if the model can accurately predict hourly indoor dry-bulb temperatures. Two samples of datasets were used here. Input datasets covering a typical summer week (15th to 22nd of June 2010) and the heat wave in July 2010 (5th to 8th of July 2010) were used for level 1 simulation. The input datasets which were used in this level of simulation had been included for developing the models and finding the best fit line.

As explained above, the models were obtained from the datasets of the units which are located in zone (a). However, the simulated results are supposed to be extended to the whole city (not only one specific building). Therefore, for a better evaluation, in addition to the simulated results, the corresponding minimum and maximum indoor dry-bulb temperatures are also presented in the following figures. In other words, the simulated

indoor dry-bulb temperatures are not supposed to be compared with hourly indoor dry-bulb temperatures of one specific unit in zone (a). Therefore, for the better evaluation of prediction ability of each model, their output results would be compared to corresponding maximum and minimum indoor dry-bulb temperature of datasets related to zone (a). Also, the variations of the results about maximum and minimum indoor dry-bulb temperatures of zone (a) units were calculated to make the evaluation easier.

Figure 5.1 shows simulated indoor dry-bulb temperatures by the time series model for the period June 15th to June 22nd 2010 with its corresponding maximum and minimum indoor dry-bulb temperatures. The variation of simulated results about maximum and minimum indoor dry-bulb temperatures are 2.27 °C and 2.31 °C, respectively for the whole datasets of months June, July, and August 2010. This implies how far the simulated results lie from the maximum and minimum indoor dry-bulb temperatures on average. It is clear that the model can accurately predict the indoor dry-bulb temperatures of a typical summer day.

Figure 5.2 represents simulated indoor dry-bulb temperatures by the time series model during the heat wave of July 5th to 8th 2010 and its corresponding maximum and minimum indoor dry-bulb temperatures. On the contrary of a typical summer day, the model was not able to predict the heat wave. As it is shown, the majority of predicted indoor dry-bulb temperatures are less than the minimum indoor dry-bulb temperatures in that period of the time.

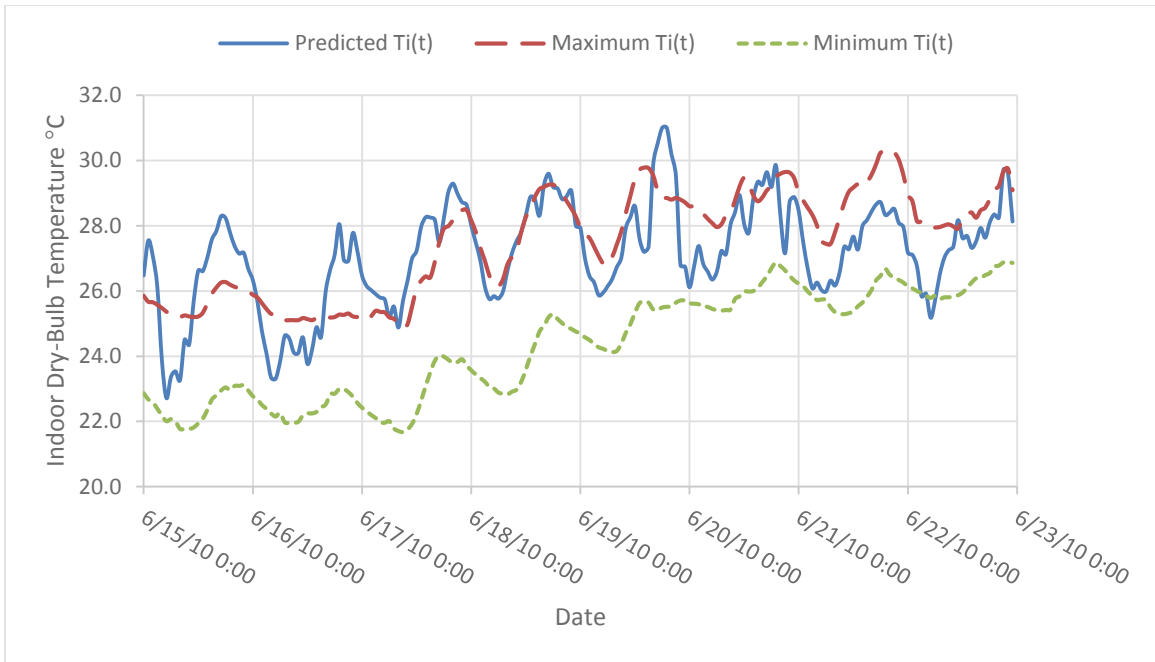


Figure 5.1 Simulated hourly indoor dry-bulb temperatures of units in zone (a)

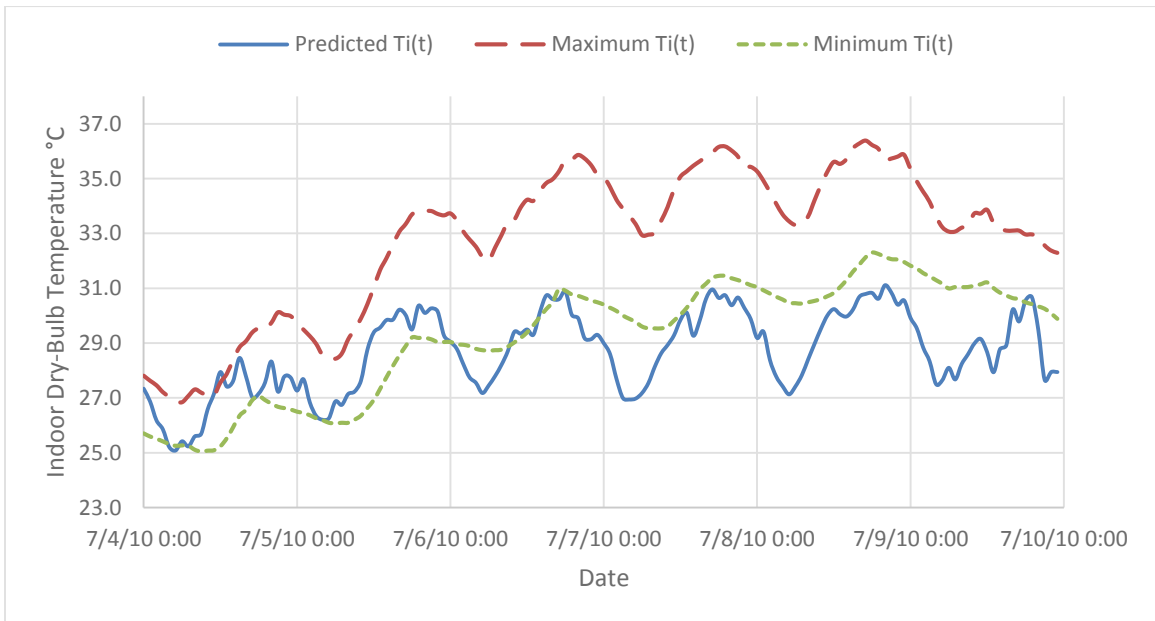


Figure 5.2 Simulated hourly indoor dry-bulb temperatures of units in zone (a)

5.1.3 Level 2 Simulation

In this level of simulation, the models were used to simulate hourly indoor dry-bulb temperatures of first eight days of August 2010: A heat wave occurred on the first three days. This dataset had not been used in the development and finding the best fit line of the models. This simulation level is the final stage for model validation, since it generates results based on totally unknown information.

Prediction results of the time series model are illustrated in Figure 5.3. Again, the model was not able to predict the indoor air temperature well during heat wave. However, it predicted relatively well the indoor dry-bulb temperatures during other periods. The variation of predicted results about maximum and minimum indoor dry-bulb temperatures are 3.39 °C and 2.23 °C, respectively.

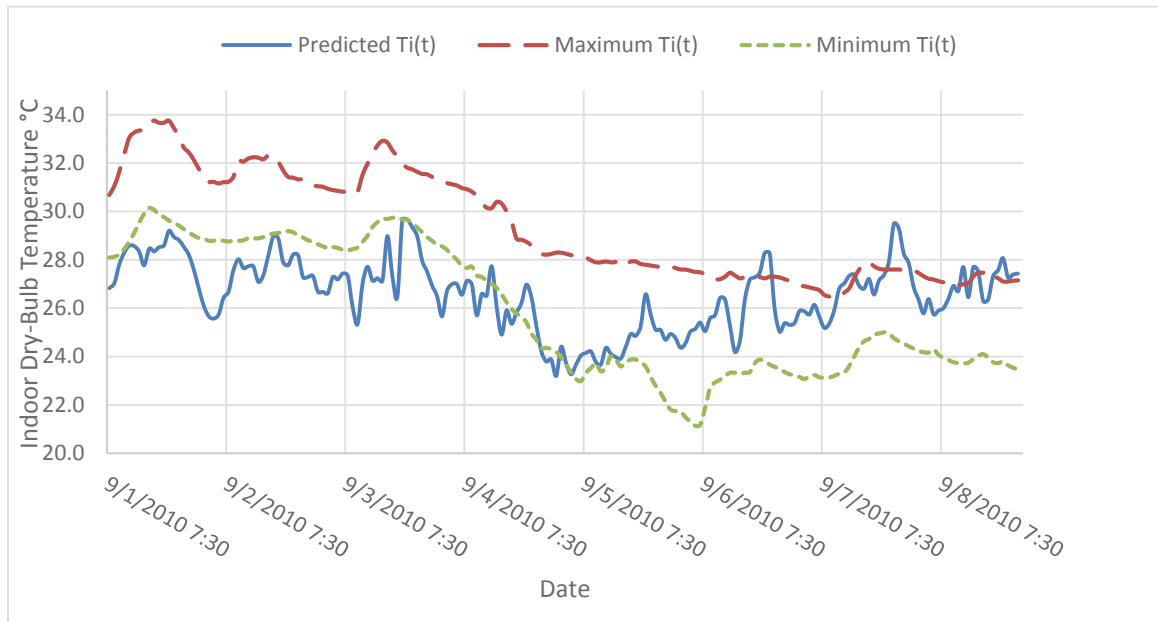


Figure 5.3 Simulated hourly indoor dry-bulb temperatures of units in zone (a)

5.2 Artificial Neural Networks

5.2.1 Apply the method

The artificial neural network model was developed using Neural Network Toolbox of MATLAB (MATLAB, 2012). The datasets of three units (Building 25, Building 28, and Building 29) which are located in zone (a) corresponding to months June, July, and August 2010 were used for training the model. The total number of the input and output layer datasets is 6,624.

In pattern recognition problems, a neural network maps between a data set of numeric inputs and a set of numeric targets. The neural network fitting tool, which was used in this study, helped to select data, create and train a network, and evaluate its performance using mean square error. A three-layer feed-forward neural network was used to solve the fitting problem between input and output datasets. The network was trained with Levenberg-Marquardt backpropagation algorithm.

At the beginning, the input of the network was selected as sol-air temperature ($^{\circ}\text{C}$), wind speed (km/h), and outdoor relative humidity (%) and time of the day which varied from 0 to 23. Indoor dry-bulb temperatures of selected units were considered as the desired target of the network. Then, the input datasets randomly were divided up for training, validation and testing. Seventy percent of the input datasets (4636 samples) was presented to the network during training, and the network was adjusted according to its error. Fifteen percent of the input datasets (994 samples) was used to measure network generalization, and to halt training when generalization stopped improving. The rest of input datasets (994 samples) was used for testing. Testing has no effect on training and so provides an

independent measure of network performance during and after training. The number of hidden neurons was changed from 1 to 100 to get the best network, RMSE between predicted and actual indoor dry-bulb temperatures was used to evaluate the networks with different number of neurons.

Finally, the best results were obtained by implementing 10 hidden neurons. The RMSE of the best model is 1.76 °C. 75 % of the predicted indoor dry-bulb temperatures by this model had an error less than ± 2 °C while 92 % had an error less than ± 3 °C.

5.2.2 Level 1 Simulation

Figure 5.4 shows simulated indoor dry-bulb temperatures by the ANN model for the period of June 15th to June 22nd 2010 with its corresponding maximum and minimum indoor dry-bulb temperatures. The variation of simulated results about maximum and minimum indoor dry-bulb temperatures are 1.93 °C and 2.03 °C, respectively for the whole datasets of months June, July, and August 2010. This implies how far simulated results lie from the maximum and minimum indoor dry-bulb temperatures on average. It can be seen that the ANN model can accurately predict the indoor dry-bulb temperatures of a typical summer day.

Figure 5.5 illustrates the simulated indoor dry-bulb temperatures by the ANN model during the heat wave occurred in July 5th to 8th 2010 and its corresponding maximum and minimum indoor dry-bulb temperatures. In addition to a typical summer day, the model also was able to simulate the heat wave. As it is shown, the majority of predicted indoor

dry-bulb temperatures are more than the minimum indoor dry-bulb temperatures and are very close to maximum indoor dry-bulb temperatures in that period of the time.

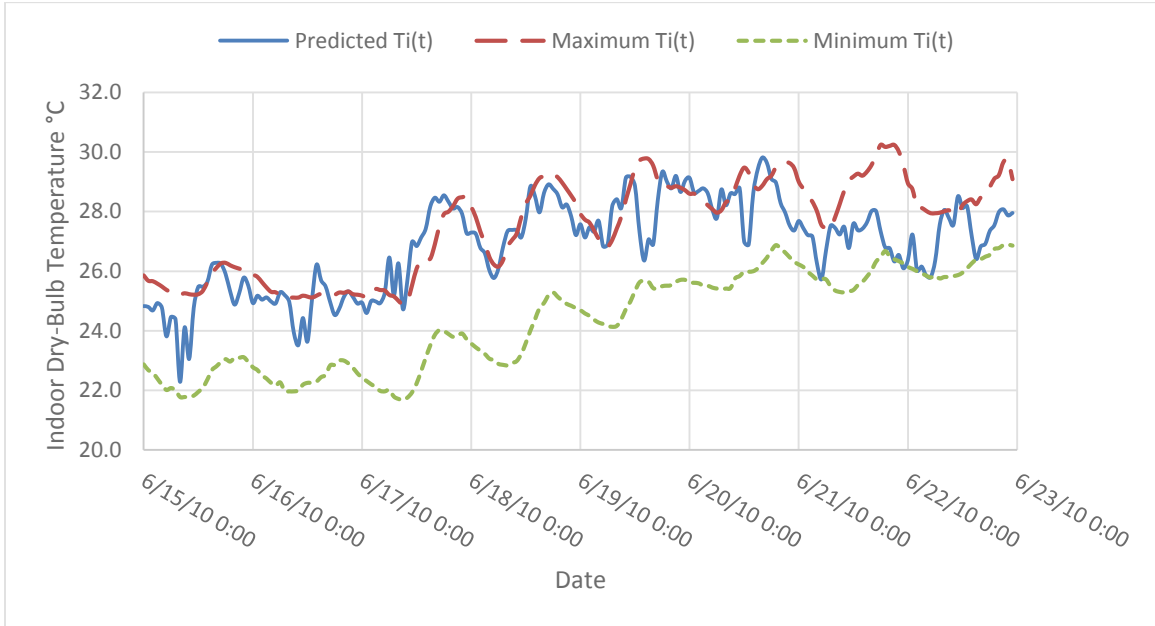


Figure 5.4 Simulated hourly indoor dry-bulb temperatures of units in zone (a) by artificial neural network model

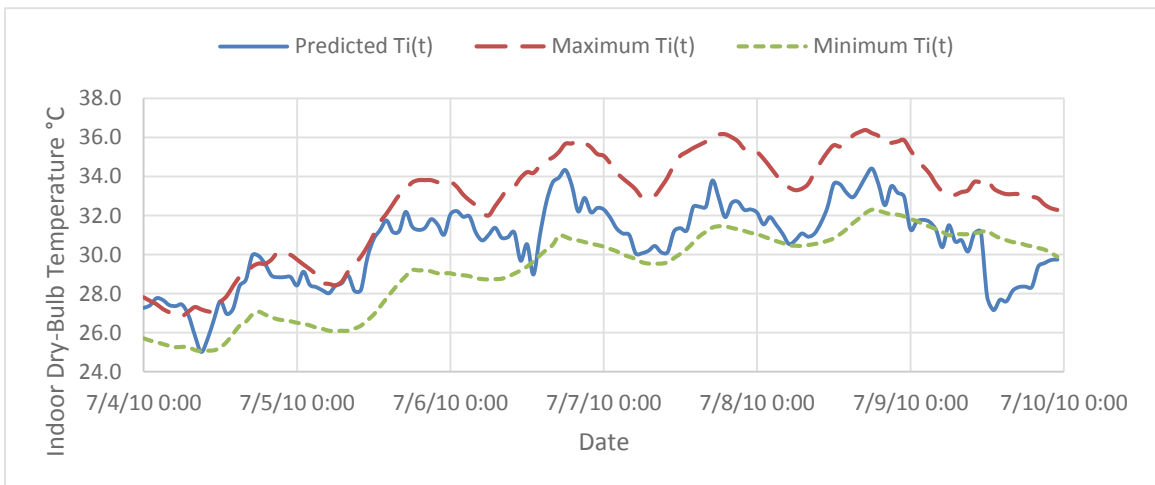


Figure 5.5 Simulated hourly indoor dry-bulb temperatures of units in zone (a) by artificial neural network model

5.2.3 Level 2 Simulation

Prediction results of the ANN model are illustrated in Figure 5.6. Again, the model was able to predict the indoor dry-bulb temperature relatively well during the heat wave and in the other time periods. The variation of predicted results about maximum and minimum indoor dry-bulb temperatures are 2.64 °C and 1.99 °C, respectively for this month.

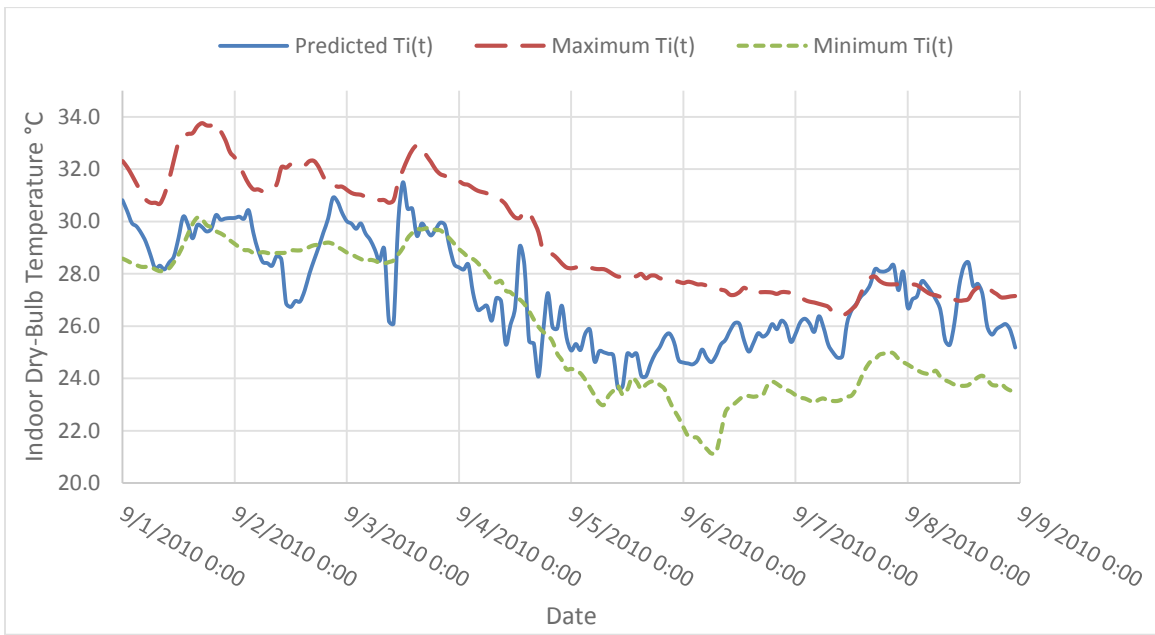


Figure 5.6 Simulated hourly indoor dry-bulb temperatures of units in zone (a) by artificial neural network model

5.3 Model Comparison

From level 1 simulation, (Figures 5.1, 5.2 (correspond to time series model) and Figures 5.4, 5.5 (correspond to ANN model)), it can be observed that both models simulated the indoor dry-bulb temperatures relatively well, with the ANN model demonstrating better accuracy. It was presented in sections 5.1.1 and 5.2.1 that the RMSE of the time series, and ANN models are 2.1 °C, and 1.76 °C, respectively. The time series model predicted indoor dry-bulb temperatures roughly 1.19 times worse than the ANN model. It is noteworthy to mention again that thirty percent of input dataset was not used during training the ANN model.

Apart from the fact that the ANN model generates less error, it should also be noted that most of the dry-bulb temperatures simulated by this model are closer or greater than the maximum indoor dry-bulb temperatures, which is an advantageous for a prediction model used as a warning system. As mentioned before, the variation of simulated results about maximum indoor dry-bulb temperatures are 2.27 °C, and 1.93 °C for the time series, and ANN models, respectively.

It was mentioned earlier that the level 2 simulation is the final stage for the warning system validation, since it predicts results based on unknown information. Figures 5.3 (corresponds to time series model), and 5.6 (Correspond to ANN model) show the results of this simulation level for all the developed models. For a better visual comparison, predicted results of both developed models correspond to level 2 simulation as well as their corresponding maximum and minimum indoor dry-bulb temperatures are shown in Figure 5.7. The ANN model generates closer prediction values with respect to the maximum and

minimum indoor dry-bulb temperatures than the time series model. The variation of simulated results about maximum indoor dry-bulb temperatures are 3.39 °C, and 2.64 °C for the time series, and ANN models, respectively.

An important observation from Figures 5.7 (and also by considering the discussed results above) is that the predictions made by the ANN model are still closer to the maximum indoor dry-bulb temperatures, reinforcing the use of this model to assess the worst case scenarios of indoor dry-bulb temperatures prediction.

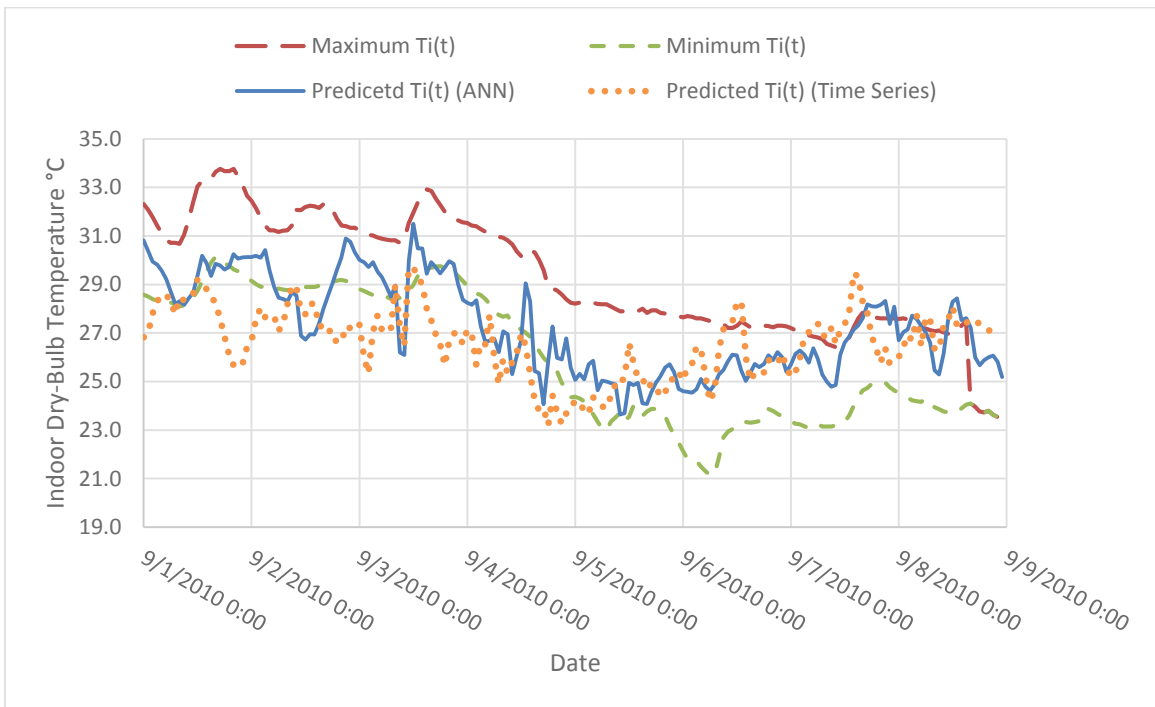


Figure 5.7 Predicated results of ANN and Time Series models correspond to simulation level 2

Chapter 6

Conclusions and Recommendations

6.1 Concluding Remarks

UHI, climate change, and global warming result in extreme heat events. They caused extensive health and economic related issues to many city residents. Elderly people living in buildings without air conditioners or mechanical ventilation systems are the most vulnerable citizens. An extensive literature review was carried out to identify the influencing parameters on indoor temperature, methods to predict indoor temperature, and existing heat warning systems. A field measurement campaign of indoor thermal condition was carried out across Montreal Island during the summer months of 2010. Fifty five dwellings were selected in different areas and various building types (Park et al., 2010). In this study, the existing measured data were used to develop predictive tools to characterize relationship between indoor dry-bulb temperatures and outdoor thermal conditions of the worst case scenario.

In order to find the worst case scenario of indoor dry-bulb temperatures during the heat waves, different building characteristic and environmental parameters were analyzed. These parameters are: building height and volume, aspect ratio, surface albedo, occupancy, sensor location, and vegetation ratio. To calculate the local wind speed and solar heat gain two models were developed. It was concluded that the top floor units in the dwellings that are located in downtown Montreal have the worst indoor thermal condition during the heat waves and were chosen as the target of this study. Measured indoor dry-bulb temperatures

related to top floor dwellings in downtown Montreal supported the conclusion about choice of worst case scenario.

The time series model consists of eleven input parameters, representing outdoor weather conditions. These parameters are current and past 8 hours observed value of sol-air temperatures (9 inputs), wind speed, and outdoor relative humidity. The ANN model consists of four inputs. They include sol-air temperature, wind speed, outdoor relative humidity, and time of the day. The output parameter of both models is the hourly indoor dry-bulb temperature. The simulation results of these two models showed that the ANN model makes a more accurate prediction of indoor dry-bulb temperatures, compared to the other model. The errors (RMSE) from the ANN model for all the levels of simulation were all smaller than those of the time series model.

Although the goal was to predict indoor dry-bulb temperature during the heat waves, in this period the developed models did not perform as well as the other periods. As it was shown before, the difference between predicted results by any of two models and the corresponding maximum indoor dry-bulb temperature was increased during the heat waves. The reason can be the limited number of days in heat waves that was used to develop models (July 5th to July 8th, 2010). Also, all the generalizations that were discussed in section 4.2 can play a role in decreasing the accuracy of the predicted results especially during the heat waves.

For developing a heat warning system, all the discussed models could be used if the benefits and limitations of each are considered. For the time series model, although it requires more input, the simulations give larger error compare to the ANN model. The

ANN model needs more expertise compare to the time series model. Moreover, developing and finding the best fit line for the ANN model is more time consuming. However, the advantages of this model greatly outweigh its drawbacks. Prediction results accuracy are noticeably increased by using this model. The good agreement between the prediction made by the ANN model and the measured data clearly demonstrated its capability of approximating any nonlinear relations even in a complex situation where some important influential parameters are unclear.

6.2 Recommendations for Future Work

The work presented in this study established a long term project in developing a heat wave alert system in the UHI. It is anticipated that more development will be performed in the future.

Apart from temperature, the thermal comfort of humans is the combined effect of other climate components such as humidity and wind speed (Leung et al., 2008). One possible way to improve the system is to predict other thermal indices which were constructed from various combination of climate components. Humidex, and Heat index are two examples of commonly used indices. It is clear that predicting indoor Humidex provides more information about indoor thermal conditions than indoor dry-bulb temperature. Conducting a more comprehensive measurement also can improve the final results. For example, knowing the internal heat generation based on the consumed electricity and gas by the occupants and aiming the top floor units in most dense area of the city for collecting data will be useful.

The neural network that was trained and used in this study is not necessarily the best possible network. Trying other learning tools, like Time Series Tool (MATLAB, 2012), may provide more accurate results.

References

- World Guides, (2013). Retrieved from http://www.montreal.world-guides.com/montreal_weather.html
- Adamowski, J., Chan, H. F., Prasher, S., Ozga-Zielinski, B., & Sliusarieva, A. (2012). Comparison of multiple linear and nonlinear regression, autoregressive integrated moving average, artificial neural network, and wavelet artificial neural network methods for urban water demand forecasting in Montreal, Canada . *Water Resources Research*, 48(1).
- Akbari, H. (2001). Cool surfaces and shade trees to reduce energy use and improve air quality in urban areas. *Solar energy*, 70(3), 295-310.
- Arnfield, A. J. (2003). Two decades of urban climate research: a review of turbulence, exchanges of energy and water, and the urban heat island. *International Journal of Climatology*, 23(1), 1-26.
- Ascione, F., Bellia, L., Capozzoli, A., & Minichiello, F. (2009). Energy saving strategies in air-conditioning for museums. *Applied Thermal Engineering*, 29(4), 676-686.
- ASHRAE Handbook - Fundamentals*. (2009). American Society of Heating, Refrigerating and Air-Conditioning Engineers, Inc. *Tullie Circle, n, e., Atlanta, GA, 30329*.
- Balaras, C., Dascalaki, E., & Gaglia, A. (2007). HVAC and indoor thermal conditions in hospital operating rooms. *Energy and buildings*, 39(4), 454-470.
- Barrow, M., & Clark, K. (1998). Heat-related illnesses. *American Family Physician*, 58(3), 749.
- Berdahl, P., & Bretz, S. (1997). Preliminary survey of the solar reflectance of cool roofing materials. *Energy and Buildings*, 25(2), 149-158.
- Bonacquisti, V., Casale, G., Palmieri, S., & Siani, A. (2006). A canopy layer model and its application to Rome. *Science of the total environment*, 364(1), 1-13.
- Bornstein, R., & Lin, Q. (2000). Urban heat islands and summertime convective thunderstorms in Atlanta: three case studies. *Atmospheric Environment*, 34(3), 507-516.
- Bottyan, Z., & Unger, J. (2003). A multiple linear statistical model for estimating the mean maximum urban heat island. *Theoretical and Applied climatology*, 75(3), 233-243.
- Bouchama, A., & Knochel, J. (2002). Heat stroke. *New England Journal of Medicine*, 346(25), 1978-1988.

- Canada Census. (2011). *Census Profile - Montreal Census Metropolitan Area*. Retrieved from Statistics Canada: <http://www.statcan.gc.ca>
- Chandler, T. J. (1966). The climate of London. *Quarterly Journal of the Royal Meteorological Society*, 320 - 321.
- Chen, H., Ooka, R., Harayama, K., Kato, S., & Li, X. (2004). Study on outdoor thermal environment of apartment block in Shenzhen, China with coupled simulation of convection, radiation and conduction. *Energy and Buildings*, 36(12), 1247-1258.
- Choices Committee on America's Climate; Council National Research. (2011). *America's Climate Choices*. The National Academies Press. Retrieved from http://www.nap.edu/openbook.php?record_id=12781
- CIBSE, T. (2005). Climate change and the indoor environment: impacts and adaptation. *Principal authors Hacker JN, Holmes MJ, Belcher SB, Davies GD*. Chartered Institute of Building Services Engineers, London.
- de Wilde, P., & Coley, D. (2012). The implications of a changing climate for buildings. *Building and Environment*.
- Ebi, K., Teisberg, T., Kalkstein, L., Robinson, L., & Weiher, R. (2004). Heat watch/warning systems save lives: Estimated costs and benefits for Philadelphia 1995-1998: Isee-165. *Epidemiology*, 14(5), S35.
- Emmanuel, R. (1997). Urban vegetational change as an indicator of demographic trends in cities: the case of Detroit. *Environment and Planning B*, 24, 415-426.
- Escourrou, G., & Pitte, J. R. (1991). *Le climat et la ville*. Nathan.
- Estournel, C., Vehil, R., Guedalia, D., Fontan, J., & Druilhet, A. (n.d.). Observations and modeling of downward radiative fluxes/Solar and Infrared/in urban/rural areas. *Journal of Climate and Applied Meteorology*, 22, 134-142.
- Fenner, R., & Ryce, T. (2008). A comparative analysis of two building rating systems. Part 1: Evaluation. *Engineering Sustainability*, 161(1), 55.
- Ferreira, P., Faria, E., & Ruano, A. (2002). Neural network models in greenhouse air temperature prediction. *Neurocomputing*, 43(1), 51-75.
- Gardner, J. (2006). Comments on 'exponential smoothing: The state of the art'. *Journal of Forecasting*, 4(1). doi:10.1002/for.3980040105

Giridharan, R., Lau, S., Ganesan, S., & Givoni, B. (2007). Urban design factors influencing heat island intensity in high-rise high-density environments of Hong Kong. *Building and Environment*, 42(10), 3669-3684.

Giridharan, R., Lau, S., Ganesan, S., & Givoni, B. (2008). Lowering the Outdoor Temperature in High-rise High-density Residential Developments of Coastal Hong Kong: The Vegetation Influence. *Building and Environment*, 43(10), 1583 - 1595. doi:10.1016/j.buildenv.2007.10.003

Givoni, B. (1998). *Climate considerations in building and urban design*. John Wiley & Sons.

Gobakis, K., Kolokotsa, D., Synnefa, A., Saliari, M., Giannopoulou, K., & Santamouris, M. (2011). Development of a model for urban heat island prediction using neural network techniques. *Sustainable Cities and Society*, 1, 104 - 115. doi:10.1016/j.scs.2011.05.001

Gouda, M., Danaher, S., & Underwood, C. (2002). Application of an artificial neural network for modelling the thermal dynamics of a building's space and its heating system. *Mathematical and Computer Modelling of Dynamical Systems*, 8(3), 333-344.

Guan, L. (2009). Preparation of future weather data to study the impact of climate change on buildings. *Building and Environment*, 44(4), 793-800.

Guan, L. (2011). Energy use, indoor temperature and possible adaptation strategies for air-conditioned office buildings in face of global warming. *Building and Environment*.

Gupta, R., & Gregg, M. (2012). Using UK climate change projections to adapt existing English homes for a warming climate. *Building and Environment*, 55, 20-42.

Hajat, S., Kovats, R. S., Atkinson, R. W., & Haines, A. (2002). Impact of hot temperatures on death in London: a time series approach. *Journal of Epidemiology and Community Health*, 56(5), 367-372.

Hajat, S., Kovats, R., & Lachowycz, K. (2007). Heat-related and cold-related deaths in England and Wales: who is at risk? *Occupational and Environmental Medicine*, 64(2), 93-100.

Health Canada. (2011). Understanding community resilience to extreme heat through table-top exercises. *Climate Change and Health: Adaption Bulletin*, 2.

Huijbregts, Z., Kramer, R., Martens, M., van Schijndel, A., & Schellen, H. (2012). A proposed method to assess the damage risk of future climate change to museum objects in historic buildings. *Building and Environment*, 55, 43-56.

Hutcheon, N. B., & Handegord, G. O. (1983). *Building science for a cold climate*. Wiley.

- Incropera, F. P., Bergman, T. L., Lavine, A. S., & DeWitt, D. P. (2006). *Fundamentals of heat and mass transfer*. John Wiley & Sons.
- Irie, B., & Miyake, S. (1988). Capabilities of three-layered perceptrons. In *Neural Networks, 1988., IEEE International Conference on* (pp. 641-648). IEEE.
- Kalkstein, L. (1993). Direct impacts in cities. *Lancet*, 342(8884), 1397-1399.
- Kalkstein, L. (2002). Description of our Heat Health Watch-Warning Systems: their nature and extend required resources. In *cCASH Workshop on Vulnerability to Thermal Stresses* (pp. 5-7).
- Kalkstein, L. S. (1999). Predicting heat worldwide. *Environmental Health Perspectives*, 107(5), A238-A244.
- Kalkstein, L. S., Jamason, P. F., Greene, J. S., Libby, J., & Robinson, L. (1996). The Philadelphia Hot Weather-Health Watch/Warning System: Development and Application, Summer 1995. 77(7), 1519-1528. doi:10.1175/1520-0477(1996)077<1519:TPHWHW>2.0.CO;2
- Kalkstein, L., & Davis, R. (2005). Weather and human mortality: an evaluation of demographic and interregional responses in the United States. *Annals of the Association of American Geographers*, 79(1), 44-64.
- Kalkstein, L., & Greene, J. (1997). An evaluation of climate/mortality relationships in large US cities and the possible impacts of a climate change. *Environmental health perspectives*, 105(1), 84.
- Kalkstein, L., & Valimont, K. (1986). An evaluation of summer discomfort in the United States using a relative climatological index. *Bull Am Meteorol Soc*, 67(7), 842-848.
- Kalkstein, L., Sheridan, S., & Au, Y. (2008). A new generation of heat/health warning systems for Seoul and other major Korean cities. *Meteorological Technology and Policy*, 1, 62-68.
- Kalkstein, L., Sheridan, S., & Kalkstein, A. (2009). Heat/Health Warning Systems: Development, Implementation, and Intervention Activities. *Biometeorology for Adaptation to Climate Variability and Change*, 33-48.
- Kalogirou, S. (2000). Applications of artificial neural-networks for energy systems. *Applied Energy*, 67(1), 17-35.
- Kilbourne, E. (1997). Heat waves and hot environments. *The public health consequences of disasters*, 245-269.

- Kim, Y.-H., & Baik, J.-J. (2002). Maximum Urban Heat Island Intensity in Seoul. *Journal of Applied Meteorology*, 41(6), 651-659. doi:10.1175/1520-0450(2002)041<0651:MUHIII>2.0.CO;2
- Kolokotroni, M., Zhang, Y., & Wa, R. (2007). The London Heat Island and building cooling design. *Solar Energy*, 81(1), 102 - 110. doi:10.1016/j.solener.2006.06.005
- Kosatsky, T., King, N., & Henry, B. (2005). How Toronto and Montreal (Canada) respond to heat. *Extreme Weather Events and Public Health Responses*, 167-171.
- Lam, C.-Y. (2010). On climate changes brought about by urban living. *Designing high-density cities for social and environmental sustainability*, 55-61.
- Landsberg, H. (1981). *The urban climate* (Vol. 28). Academic press Inc. Fifth Avenue, New York, New York 10003
- Lankester, P., & Brimblecombe, P. (2012). Future thermohygro-metric climate within historic houses. *Journal of Cultural Heritage*, 13(1), 1 - 6.
- Leung, Y., Yip, K., & Yeung, K. (2008). Relationship between thermal index and mortality in Hong Kong. *Meteorological Applications*, 15(3), 399-409.
- Liu, Y., Zhou, C.-F., & Chen, Y.-W. C. (2006). Weight Initialization of Feedforward Neural Networks by Means of Partial Least Squares., (pp. 3119-3122). doi:10.1109/ICMLC.2006.258402
- Lowry, G., & Lee, M. (2004). Modelling the passive thermal response of a building using sparse BMS data. *Applied energy*, 78(1), 53-62.
- Lu, T., & Viljanen, M. (2009). Prediction of indoor temperature and relative humidity using neural network models: model comparison. *Neural computing & applications*, 18(4), 345-357.
- Lun, I., Ohba, M., & Morikami, S. (2012). An Overview of Extreme Hot Weather Incidents and the Role of Natural Ventilation in Buildings on Human Body Comfort. *International Journal of Ventilation*, 11(3), 311-322.
- Makridakis, S. G. (1983). Empirical evidence versus personal experience. *Journal of Forecasting*, 295-306.
- MATLAB. (2012). R2012b math works documentation. Math Work Inc.
- Mavrogianni, A. a., Wilkinson, P., Kolokotroni, M., & Milner, J. (2009). Space heating demand and heatwave vulnerability: London domestic stock. *Building Research & Information*, 37(5-6), 583-597.

- Mavrogianni, A., Wilkinson, P., Davies, M., Biddulph, P., & Oikonomou, E. (2012). Building characteristics as determinants of propensity to high indoor summer temperatures in London dwellings. *Building and Environment* 55, 117-130.
- Mechaqrane, A., & Zouak, M. (2004). A comparison of linear and neural network ARX models applied to a prediction of the indoor temperature of a building. *Neural Computing & Applications*, 13(1), 32-37.
- Microsoft. (2013). Microsoft Excel [computer software]. Redmond, Washington. Retrieved from <http://office.microsoft.com/en-ca/excel/>
- Mihalakakou, G., Flocas, H. A., Santamouris, M., & Helmis, C. G. (2002). Application of Neural Networks to the Simulation of the Heat Island over Athens, Greece, Using Synoptic Types as a Predictor. *Journal of Applied Meteorology*, 41(5).
- Mirzaei, P., & Haghighat, F. (2010). Approaches to study urban heat island--abilities and limitations. *Building and Environment*, 45(10), 2192-2201.
- Mirzaei, P., & Haghighat, F. (2012). A procedure to quantify the impact of mitigation techniques on the urban ventilation. *Building and Environment*, 47, 410-420.
- Mirzaei, P., Haghighat, F., Nakhaie, A., Yagouti, A., Keusseyan, R., & Coman, A. (2012). Indoor thermal condition in urban heat island-development of a predictive tool. *Building and Environment*, 57, 7-17.
- Mochida, A., Tabata, Y., Iwata, T., & Yoshino, H. (2008). Examining tree canopy models for CFD prediction of wind environment at pedestrian level. *Journal of Wind Engineering and Industrial Aerodynamics*, 96(10), 1667-1677.
- Montgomery, D. C. (2009). *Introduction to Statistical Quality Control* (6th ed.). WILEY.
- Muth, J. F. (1960). Optimal properties of exponentially weighted forecasts. *Journal of the American Statistical Association*, 299-306.
- Nakai, S., Itoh, T., & Morimoto, T. (1999). Deaths from heat-stroke in Japan: 1968-1994. *International Journal of Biometeorology*, 43(3), 124-127.
- National Climate Data and Information Archive. (2012, 03 24). *Canadian Climate Normals 1971-2000*. Retrieved from National Climate Data and Information Archive: <http://www.climate.weatheroffice.gc.ca>
- NOAA. (1994). *Regional Operations Manual Letter. Eastern Region National Weather Service*. Bohemia, NY.

- NWS. (1992). Non-precipitation weather hazards. *Weather Service Operations Manual*, 92(5), 5.
- Oikonomou, E., Davies, M., Mavrogianni, A., Biddulph, P., Wilkinson, P., & Kolokotroni, M. (2012). Modelling the relative importance of the urban heat island and the thermal quality of dwellings for overheating in London. *Building and Environment*, 57, 223-238.
- Oke, T. R. (1992). *Boundary layer climates*. Psychology Press.
- Oke, T. R., & East, C. (1971). The urban boundary layer in Montreal. *Boundary-Layer Meteorology*, 1(4), 411-437.
- Oke, T. R., Spronken-Smith, R. A., Jauregui, E., & Grimmond, C. S. (1999). The energy balance of central Mexico City during the dry season. *Atmospheric Environment*, 33(24), 3919-3930.
- Pachauri, R., & Reisinger, A. (2007). *Contribution of Working Groups I, II and III to the Fourth Assessment Report of the Intergovernmental Panel on Climate Change*. Geneva, Switzerland.
- Park, H. (1986). Features of the heat island in Seoul and its surrounding cities. *Atmospheric Environment (1967)*, 20(10), 1859-1866.
- Park, K.-W., Akbari, H., & Haghghat, F. (2010). *Measuring and Modeling Indoor Thermal Conditions in Urban Heat Island Areas: The Case of Montreal Island*. Montreal.
- Pedrini, A., Westphal, F., & Lamberts, R. (2002). A methodology for building energy modelling and calibration in warm climates. *Building and Environment*, 37(8-9), 903 - 912. doi:10.1016/S0360-1323(02)00051-3
- Pollard, A., & Stoecklein, A. (1998). Occupant and building related determinants on the temperature patterns in New Zealand residential buildings. *IPENZ Conference 98: The sustainable city; Volume 2; Electrotechnical : simulation and control; energy management : telecommunications*, (p. 62). Wellington. Retrieved from <http://search.informit.com.au/documentSummary;dn=425987970518989;res=IELENG>
- Porritt, S., Shao, L., Cropper, P., & Goodier, C. (2010). Building orientation and occupancy patterns and their effect on interventions to reduce overheating in dwellings during heat waves. Institute of Energy and Sustainable Development (IESD)
- Priyadarsini, R., Hien, W. N., & David, C. (2008). Microclimatic modeling of the urban thermal environment of Singapore to mitigate urban heat island. *Solar Energy*, 82, 727 - 745. doi:10.1016/j.solener.2008.02.008

- Rooney, C., McMichael, A., Kovats, R., & Coleman, M. (1998). Excess mortality in England and Wales, and in Greater London, during the 1995 heatwave. *Journal of epidemiology and community health*, 52(8), 482-486.
- Ruano, A., & Crispim, E. (2006). Prediction of building's temperature using neural networks models. *Energy and Buildings*, 38(6), 682-694.
- Sailor, D., & Dietsch, N. (2007). The urban heat island mitigation impact screening tool (MIST). *Environmental Modelling & Software*, 22(10), 1529-1541.
- Sarrat, C., Lemonsu, A., Masson, V., Guedalia, D. (2005). Impact of urban heat island on regional atmospheric pollution. *Science Direct*, 40(10), 1743 - 1758.
- Schuman, S. (1972). Patterns of urban heat-wave deaths and implications for prevention: data from New York and St. Louis during July, 1966. *Environmental Research*, 5(1), 59-75.
- Semenza, J., McCullough, J., Flanders, W., McGeehin, M., & Lumpkin, J. (1999). Excess hospital admissions during the July 1995 heat wave in Chicago. *American journal of preventive medicine*, 16(4), 269-277.
- Shao, B., Zhang, M., Mi, Q., & Xiang, N. (2011). Prediction and Visualization for Urban Heat Island Simulation. In *Transactions on Edutainment VI* (pp. 1-11). Springer Berlin / Heidelberg. Retrieved from http://dx.doi.org/10.1007/978-3-642-22639-7_1
- Shashua-Bar, L., Hoffman, M., & Tzamir, Y. (2006). Integrated thermal effects of generic built forms and vegetation on the UCL microclimate. *Building and environment*, 41(3), 343-354.
- Sheridan, S., & Kalkstein, L. (1998). Heat watch-warning systems in urban areas. *World Resource Review*, 10(3), 375-383.
- Sheridan, S., & Kalkstein, L. (2004). Progress in heat watch-warning system technology. *Bulletin of the American Meteorological Society*, 85(12), 1931-1942.
- Smoyer, K. (1998). A comparative analysis of heat waves and associated mortality in St. Louis, Missouri-1980 and 1995. *International Journal of Biometeorology*, 42(1), 44-50.
- Smoyer-Tomic, K., & Rainham, D. (2001). Beating the heat: development and evaluation of a Canadian hot weather health-response plan. *Environmental health perspectives*, 109(12), 1241.
- Statistics Canada. (2011). Retrieved from <http://www12.statcan.gc.ca>.

- Steadman, R. (1979). The assessment of sultriness. Part I: A temperature-humidity index based on human physiology and clothing science. *Journal of Applied Meteorology*, 18(7), 861-873.
- Tan, J., Kalkstein, L., Huang, J., Lin, S., Yin, H., & Shao, D. (2004). An operational heat/health warning system in shanghai. *International Journal of Biometeorology*, 48(3), 157-162. doi:10.1007/s00484-003-0193-z
- Tham, Y. W., & Muneer, T. (2011). Sol-air temperature and daylight illuminance profiles for the UKCP09 data sets. *Building and Environment*, 46(6), 1243-1250.
- Thomas, B., & Soleimani-Mohseni, M. (2007). Artificial neural network models for indoor temperature prediction: investigations in two buildings. *Neural Computing & Applications*, 16(1), 81-89.
- UKCIP. (2010, September). *Climate digest*. Retrieved from <http://www.ukcip.org.uk/climate-digest/>
- Vandentorren, S., Bretin, P., Zeghnoun, A., Mandereau-Bruno, L., Croisier, A., Cochet, C., . . . Ledrans, M. (2006). August 2003 heat wave in France: risk factors for death of elderly people living at home. *The European Journal of Public Health*, 16(6), 583-591.
- Wei, S., Sun, Y., Li, M., Lin, W., Zhao, D., Shi, Y., & Yang, H. (2011). Indoor thermal environment evaluations and parametric analyses in naturally ventilated buildings in dry season using a field survey and PMVe-PPDe model. *Building and Environment*, 46(6), 1275-1283.
- Wilhelmi, O., Purvis, K., & Harriss, R. (2004). Designing a Geospatial Information Infrastructure for Mitigation of Heat Wave Hazards in Urban Areas. *Natural Hazards Review*, 147-158.
- Wright, A., Young, A., & Natarajan, S. (2005). Dwelling temperatures and comfort during the August 2003 heat wave. *Building Services Engineering Research and Technology*, 26, 285-300. doi:10.1191/0143624405bt136oa
- Wu, S., & Sun, J. (2012). Multi-stage regression linear parametric models of room temperature in office buildings. *Building and Environment*, 56, 69 - 77.
- Yan, D., Song, F., Yang, X., Jiang, Y., Zhao, B., Zhang, X., . . . Wu, P. (2008). An integrated modeling tool for simultaneous analysis of thermal performance and indoor air quality in buildings. *Building and Environment*, 43(3), 287-293.
- Zhang, Q., Wong, Y., Fok, S., & Bong, T. (2011). Neural-based air-handling unit for indoor relative humidity and temperature control. *ASHRAE Transactions*, 111(1), 63-70.